BABES-BOLYAI UNIVERSITY
FACULTY OF PHYSICS

DIANA-LOUISA TRANDAFIR

THE STUDY OF SOME NANOSTRUCTURATED SILICA-GERMANATE SYSTEMS

PhD Thesis Summary

Scientific Supervisor:

Prof. Dr. Simion SIMON

Cluj-Napoca, 2011

BABES-BOLYAI UNIVERSITY

FACULTY OF PHYSICS

DIANA-LOUISA TRANDAFIR

THE STUDY OF SOME NANOSTRUCTURATED SILICA-GERMANATE SYSTEMS

PhD Thesis Summary

Scientific Supervisor:

Prof. Dr. Simion SIMON

Cluj-Napoca, 2011

CONTENTS

Keywords

Sol-gel, spray-drying, nanocrystals, DTA, XRD , IR, Raman, ^{29}Si MAS-NMR.

Introduction

The purpose of this thesis is to synthesis by sol gel method oxide materials of scientific interest with properties exploited different applications.

Glass is one of the oldest material, a long time being used only for decorative purposes, but areas where the glasses found their applicability has expanded considerably with the technological progress and theoretical concepts. In recent years new applications have emerged (lasers, fiber optics, semiconductor devices, photosensitive storage of radioactive waste, etc...) in different fields (construction, transportation, lighting, etc...) where this class of materials bring original solutions besides the classical applications, in which glasses are indispensable to a modern economy. To extend as far as the applicability scope of oxide materials with vitreous structure should be investigate their structures, a determining factor in material properties. Vitreous materials or glasses are non-crystalline materials obtained by different methods, whose main characteristic is the absence of long-distance order. In terms of local order include the full range of vitreous material between the amorphous ones, characterized by an extremely broad distribution of the fundamental structural unit and ceramic materials obtained by partial characterization of glasses and where can be find both features of the vitreous and polycrystalline materials. To understand and control the properties of different glassy materials whose application areas are in constant development, great importance is the knowledge of the local structure in such disordered systems, the way in which different technological factors that intervene in their production process influences the type, structure and share the various structural units whose chaotic interconnection make the vitreous network.

Silicon has many industrial applications as the main component of most semiconductor devices, the most important being integrated circuits and microchips. Silicon is widely used in semiconductors because it remains semiconducting at higher temperatures than germanium-based semiconductors and because the oxide is obtained easily and form of semiconductor/dielectric interfaces better than other combinations of materials.

SiO_2 natural oxide of silicon, is of great interest in microelectronics, as a superior insulator with high thermal and chemical stability [1, 2] and is the largest component of glass, or silicates, quartz being the most representative. It is used in various fields, from the manufacture of paints, varnishes, adhesives, art, the semiconductor industry, in pharmaceuticals, cosmetics, food or the particular layers of pigment in paper production. It has also a great importance in the glass, lens optical devices as electrically insulating, laboratory quartz glass is almost indispensable. Silicate glasses obtained by sol-gel is a promising alternative in the production of new medical devices with specific properties, their advantage is the high degree of purity, high specific surface and high homogeneity, the presence of hydroxyl groups and high degree of porosity leading to high reactivity .

GeO_2 glass is used to obtain glasses in a new range of applications especially as part of the optical semiconductor devices for integrated circuits and transistors. Because of relatively high refractive index and its optical dispersion properties is used as material for optical lenses optical microscopes objectives.

Silicate and germanate glasses are among the most studied oxide glasses and are considered classics glasses, the both network formers have a similar structure despite differences between the bonds length and angles between them and also for the relative size of germanium atoms to those of silicon.

There were intensely studied glasses and vitroceramics belonging to the SiO_2-M_2O (M=Li, Na, K), SiO_2-MO (M=Be, Mg, Ca, Sr, Ba), SiO_2-M_2O_3 (M=B, Al, Ga), SiO_2-MO_2 (M=Ti, Zr, Sn) and SiO_2-M_2O_5 (M=P, Bi) binary systems. But there are only few studies on non-crystalline and partially crystalline materials belonging to the SiO_2-GeO_2 system probably due to the difficulties in preparing the glasses belonging to this system by the classical method, especially in areas with high concentration of germanium. The system consists of the two oxides is recognized as a distinct properties including strength, purity and economic accessibility in obtaining new optical properties for optical waveguides and other applications. In the case of SiO_2 and GeO_2, it was observed that the gradual replacement of silicon dioxide with germanium dioxide or other oxides, in various types of glass, increase their refractive index. To obtain such devices is needed but full characterization of the structural and optical properties of materials.

Although silica-germanate glasses have been extensively studied in the literature are important disagreements and conflicting data, important details of structure and composition remain unclear [1-7].

The sol-gel materials can be prepared at low temperature with high purity and homogeneity; the possibility of obtaining non-crystalline materials with controlled structure and composition have made the sol-gel process a possible encapsulation technique for therapeutic applications of isotopes.

High porosity and surface area associated with the typical structure of xerogel produced by this method allows obtaining materials with active surfaces and different rates of degradation. Spray drying of sol allows to obtain microspheres with desired size.

The thesis is structured in three chapters and aims in terms of structural characterization of non-crystalline compounds in the system SiO_2-GeO_2 doped with gadolinium, prepared by sol-gel and spray drying methods and the changes induced by heat treatments in these compounds. The first chapter presents the methods for obtaining materials, sol-gel and spray drying methods. The second chapter summarizes the methods used to investigate materials: differential thermal and thermogravimetric analysis, X-ray diffraction, Raman and Infrared spectroscopies, nuclear magnetic resonance.

The third chapter includes the experimental results obtained for both materials obtained by sol-gel method and those obtained by spray drying method, followed by conclusions, bibliography and appendices.

1. SAMPLE PREPARATION

The 0.995 •[(1-x)SiO_2 • xGeO_2]• 0.005Gd_2O_3 systems was studied, obtaining samples with different values of ratio Si/Ge (Table 1), the amount of gadolinium being constant. There were been prepared two sets of samples, one obtained by sol-gel method and the other by spray drying. The tetraethil-ortosilicate $Si(OC_2H_5)_4$ (TEOS), germanium ethoxide $Ge(OC_2H_5)_4$ (TEOG), gadolinium nitrate hexahydrate $Gd(NO_3)$ • $6H_2O$ of high purity were used as precursors.

The solvent used was ethanol and HCl was used as catalyst. Figure 1.1 is a schematic diagram of preparation process and the processing parameters for the spray drying procedure are presented in the next table.

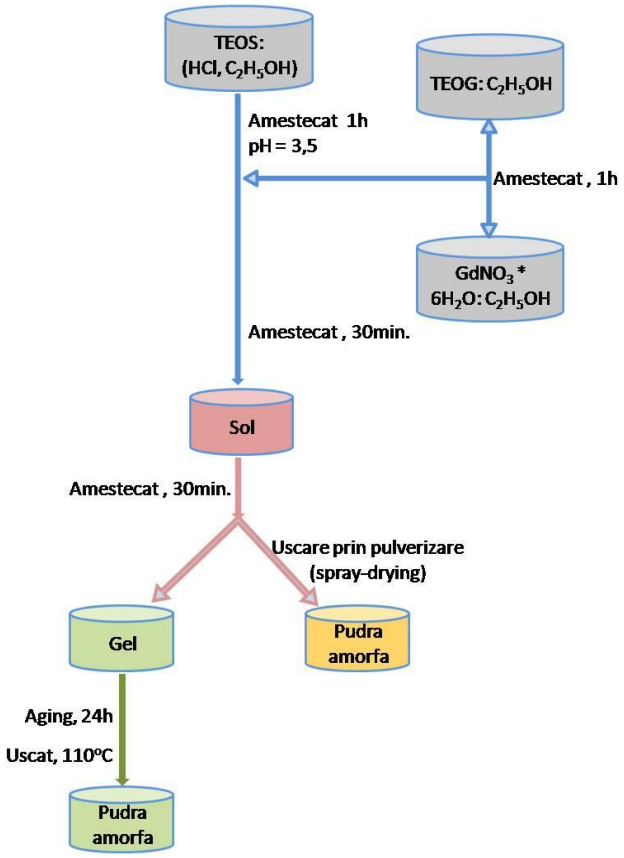

Figure 1.1. Schematic diagram of preparation process.

Table 1.

0.995·[(1-x)SiO_2 · xGeO_2]·0.005Gd_2O_3 system

Si/Ge	1-x (SiO_2)	x (GeO_2)		
8:1	0.889	0.111		
6:1	0.858	0.142		
4:1	0.8	0.2		
2:1	0.667	0.333		
1:1	0.5	0.5		
1:3	0.25	0.75		
1:4	0.2	0.8		
Spray parameters				
Pump (%)	Asp (%)	Flow (l/h)	T_{in} / T_{out} (°C)	
16	95	50	95 / 50	

All samples were obtained at room temperature and spray parameters were the same for all samples prepared.

2. EXPERIMENTAL RESULTS FOR THE 0.995 •[(1-X)SiO_2 • XGeO_2]• 0.005•Gd_2O_3 SYSTEM OBTAINED BY SOL-GEL PROCESS

2.1. Thermal analysis results

Thermal analysis curves for the samples obtained by sol-gel process revealed the removes water and other organic components temperatures and also the others thermal events that occur in the samples.

The TGA curves obtained can easily identify the mass loss taking place in two steps, accompanied in DTA curves by endo-or exothermal effects. The first step of mass loss that occurs in the range 20-250^oC DTA curve is accompanied by an endothermic effect which is attributed to elimination of adsorbed water and solvent, in this case of alcohol. The second step of mass loss in 250-500^oC range, indicating a decomposition of the organic part from the silica matrix, elimination and decomposition of nitrates and chlorides is accompanied on the DTA curve by exothermic effects [8-13].

For samples with higher silicon content (samples with the ratio Si/Ge 8:1-2:1), the exothermic peaks in the range 900-1100^oC correspond to a phase transition, probably a beginning of crystallization and there are not accompanied by weight loss in TGA curve. For samples with a high germanium content (sample with the ratio Si/Ge 1:1-1:4) the phase transition peak is not observed.

In the figure 2.1 are presented the curves of thermal analysis for the samples obtained by the ratio Si/Ge 2:1 and 1:1 respectively.

Following the thermal analysis have been established the heat treatment temperatures to 550^oC and 1200^oC for samples with high silicon content and 550^oC, 900^oC respectively for samples with high germanium content.

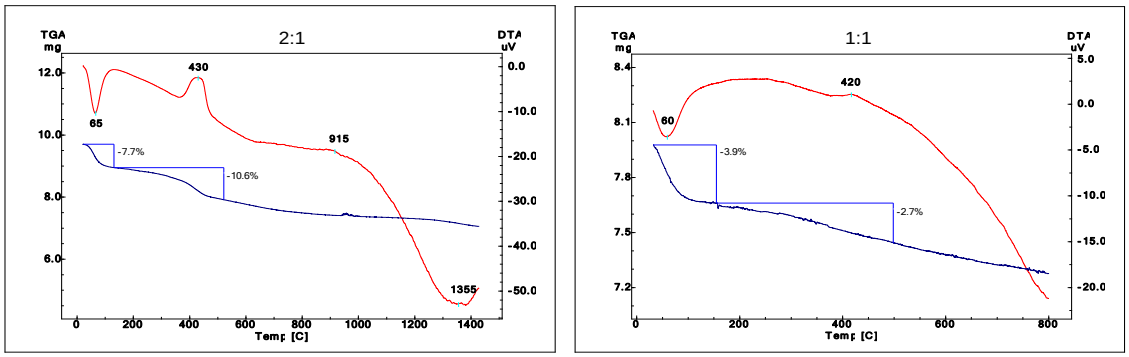

Figure 2.1. DTA and TGA curves for the sample with 2:1and 1:1 Si/Ge ratio.

2.2. Structural characterization by XRD

X-ray patterns recorded on as-prepared samples (Figure 2.2) with high silicon content, show an amorphous structure, which could be concluded from the broad characteristic diffraction peak between 2θ ~ 15° and 30°, on account of the amorphous character of as-prepared xerogels [13]. For samples with a high germanium content (the ratio of Si/Ge 1:3, 1:4 respectively) the X-ray patterns have specific features of crystalline structures, germanium oxide being the identified phase. The average crystallites size, determined by Scherrer's formula for the peak with 2θ = 25.8^{o}, was around 8 nm.

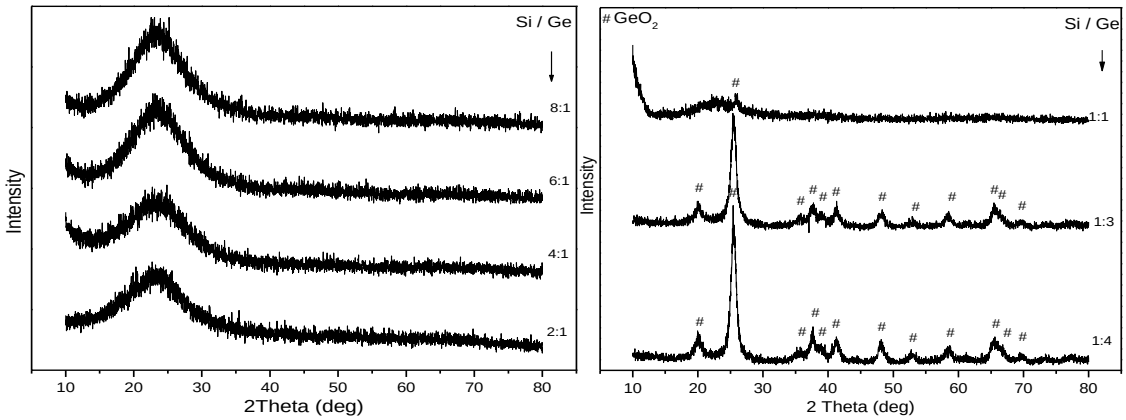

Figure 2.2. X-ray patterns for the as-prepared samples.

For the X-ray patterns recorded for 550^{o}C heat treated samples for 30 minutes (Figure 2.3), with a high silicon content, the central peak does not change the position and non-crystalline systems retain their specific features. The X-ray patterns for the samples with a high germanium content present crystalline characteristics and germanium

oxide being the identified phase. The average crystallites size, determined by Scherrer's formula for the peak with $2\theta = 26.6^{o}$, has values ranging between 24.5-8.5 nm and decreases with increasing the germanium content in the samples.

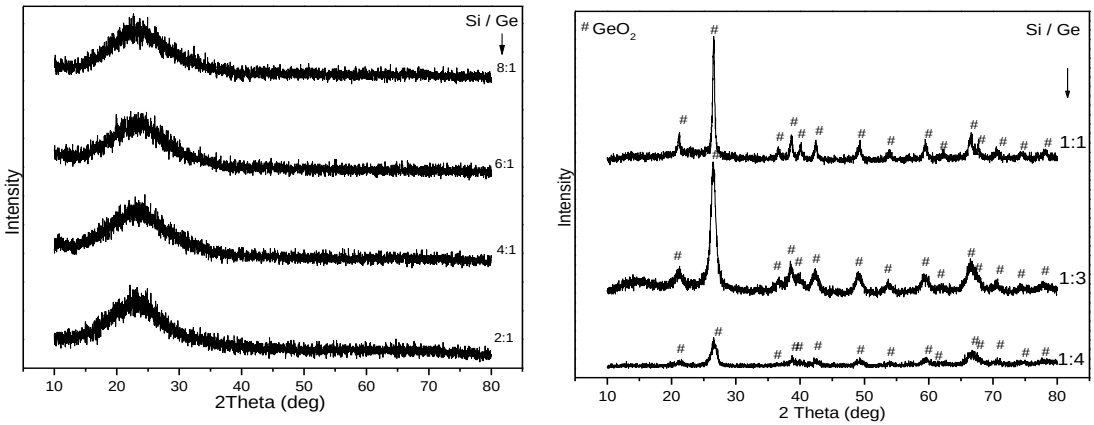

Figure 2.3. X-ray patterns for the samples 550°C heat treated for 30 minutes

X-ray patterns recorded for the 1200°C heat treated samples for 30 minutes, with a high silicon content, reflect the beginning of crystallization process maintaining a certain extent and specific features of non-crystalline systems, while the X-ray pattern of the for sample with atomic ratio Si/Ge 2:1 shows a mostly crystalline structure, α-cristobalite being the predominant phase, but also small amount of quart occured (Figure 2.4). The average crystallites size of cristobalite, determined by Scherrer's formula for the peak with $2\theta \sim 21.9^{o}$, for the partially crystallized samples is ~ 9.4 nm and decreases with the increasing of germanium content. For the crystalline sample with atomic ratio Si/Ge 2:1 the average crystallites size is arround 35 nm.

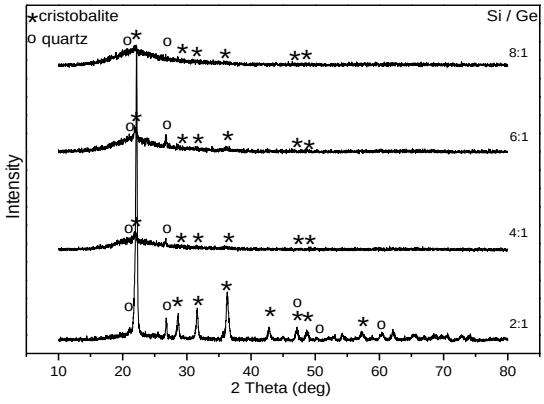

Figure 2.4. X-ray patterns for the sample with 8:1-2:1atomic ratio, 1200°C heat treated for 30 minutes.

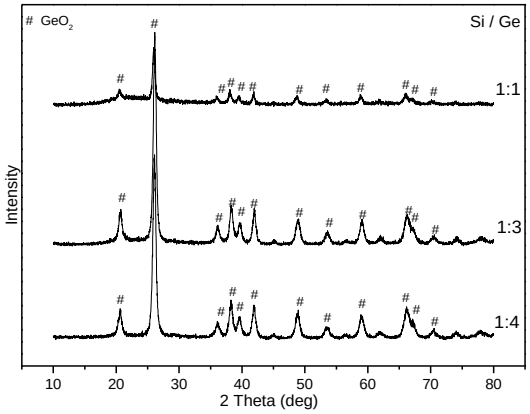

Figure 2.5. X-ray patterns for the sample with 1:1-1:4 atomic ratio, 900°C heat treated for 30 minutes

For the 900°C heat treated samples (30 minutes) with high germanium content the X-ray patterns are specific to the crystalline systems, germanium oxide being the identified phase (Figure 2.5) and the average crystallite size being around 19 nm.

X-ray patterns recorded for the 1200°C heat treated samples for 24 houres, with a high silicon content (Figure 2.6), reflect also a crystalline structure, α-cristobalite with a cubic structure being the identified phase. The average crystallites size for the samples with Si/Ge 2:1-8:1 atomic ratio has values ranging between 35-39,5 nm.

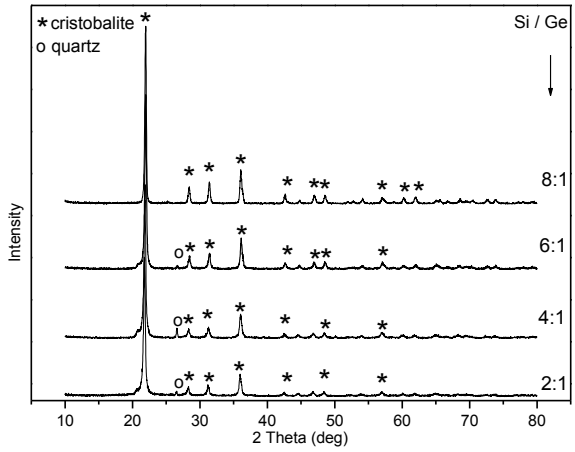

Figure 2.6. X-ray patterns for the samples 1200°C heat treated for 24hours.

2.3. Structural characterization by Raman spectroscopy

The most important features of Raman spectra were observed for the wavenumbers between 200 - 1500 cm^{-1} and 2800-3700 cm^{-1}, respectively.

The Raman spectra of as-prepared samples (Figure 2.7) were mainly identified bands typical of silica network. The broad band in the range of 430-490 cm^{-1} can be associated with the bending vibration of Si-O-Si bond [14-20] and the one between 780-830 cm^{-1} to the symmetric stretching vibrations of Si-O-Si [10, 11, 14-18, 20-22].

The band arround 880 cm^{-1} is given by the asymmetric stretching vibration of Ge-O-Ge bond in the GeO_4 tetrahedra [19, 23-28]. In the silicate glasses, the band assigned to symmetric stretching vibrations of Ge-O-Ge bond in the GeO_4 tetrahedra (~ 418 cm-1) is delocalized and has a mixed character, stretching-bending [29], so one can not exclude the contribution of this band to the one in the range of 430-490 cm^{-1}.

The band located in the 900-970 cm^{-1} range can be attributed to ν (Si-O-Ge) [19, 25-27, 30-33] and the band between 1050-1105 cm^{-1} with antisymmetric stretching

vibrations of Si-O-Si [10, 11, 14, 16-18, 20-22, 25, 26, 28, 32, 34-39]. For as-prepared samples the band arround 980 cm^{-1} attributed to Si-OH bond vibration is present in the heat treated xerogel up to ~ 800^{o}C. The disappearance of this band can be related to gel-glass transition, a process that is completed in other systems around the temperature of 400-600°C [14, 16-19, 40].

According to data reported in the literature [32, 41-47] the vibration modes arround 430 cm^{-1} and 1000-1200 cm^{-1} can be associated with Q^4 units, the ones arround 490 $cm^{-1}$with Q^3 units and the ones in 900-980 cm^{-1} range with Q^3 and Q^2 units, respectively.

The Raman bands in 1300-1465 cm^{-1} range are assigned to bending vibrations of C-H bond [11, 14, 48], the ones in 2890-2990 cm^{-1} range to the stretching vibration of C-H bond [10, 11, 14, 16, 17, 33, 34, 36, 37, 48-51] and the ones between 3430-3450 cm^{-1} to the stretching vibrations ν (OH) [18-30, 48].

The Raman spectra of the samples with high germanium content (the atomic ratio Si/Ge 1:1-1:4) present a fluorescence phenomena witch cover the Raman signal.

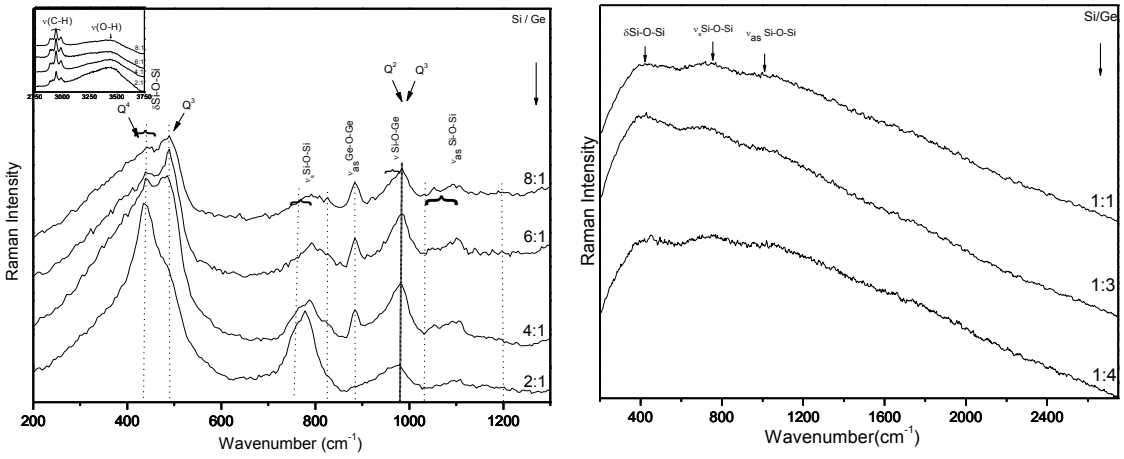

Figure 2.7. Raman spectra for the as-prepared samples.

In the case of 550^{o}C heat treated (30 minutes) samples (Figure 2.8) some bands don't occuered comparing with as-prepared ones. In these spectra were also identified typical bands of silica network in the 1020-1190 cm^{-1}, 775-830 $cm^{-1}$and 430-490 cm^{-1} spectral ranges associated with symmetric, antisymmetric stretching and bending of the Si-O-Si vibrations modes, respectively [10, 11, 14-22, 25, 31, 35, 36, 38, 52].

The decreasing in intensity with the thermal treatment up to 550^{o}C for the band arround 885 cm^{-1}, attributed to asymmetric stretching vibration of Ge-O-Ge bond in GeO^4 [19, 23-26, 29] shows a better insertion of germanium into amorphous silicate network. The bands in 1300-1465 cm^{-1} range attributed to δ (C-H) and ν (C-H) vibration disappears after termal treatment at 550°C, which follows from the differential thermal analysis. The bands between 3420-3440 cm^{-1} attributed to O-H vibration, ν(O-H) [18, 27, 30, 34, 39, 48, 51] are still present in the samples. In the Raman spectra of 550^{o}C heat treated sample with high germanium content (the atomic ratio Si/Ge 1:1-1:4), the fluorescence phenomena still occures and covers the Raman signal.

Similar with the Raman spectra analysis of the as-prepared samples, modes of vibration at 430 cm^{-1} and 1000-1200 cm^{-1} may be associated with units Q^4, those at 490 cm^{-1} with Q^3 units and modes of vibration in the range 900 - 980 cm^{-1} with Q^3 and Q^2 units [32, 41-47].

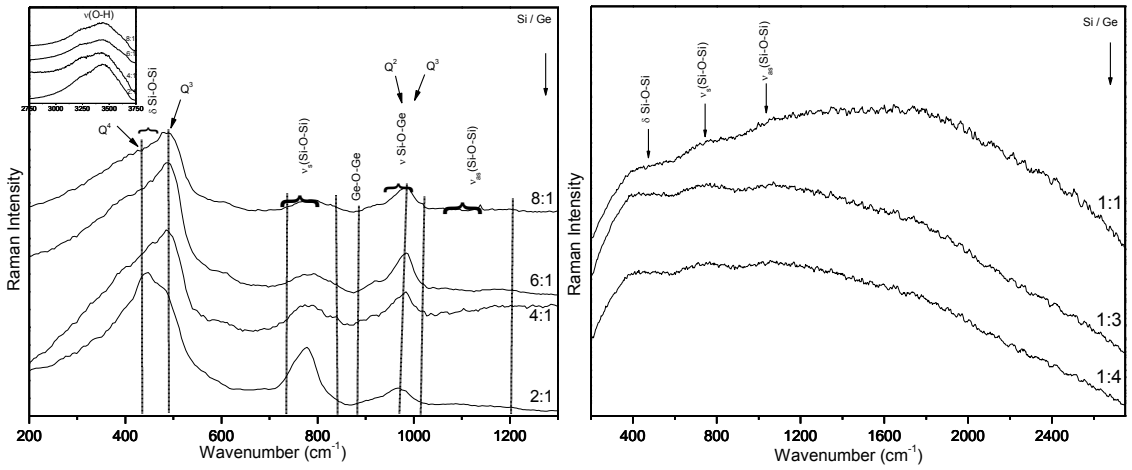

Figure 2.8. Raman spectra for the heat treated samples at 550^{o}C for 30 minutes.

In the case of Raman spectra for the 1200^{o}C heat treatment (30 minutes) samples with high silicon content (Figure 2.9) can be seen the typical silica network bands atributed to the symmetric, antisymmetric stretchings and bending vibrations of the Si-O-Si bond, the spectral range of 1020-1200 cm^{-1}, 800-810 cm^{-1} and 430-490 cm^{-1} respectively [10, 11, 14-19, 21, 22, 34, 36-39, 52**]**.

The band at 885 cm^{-1} attributed to antisymmetric stretching vibration of Ge-O-Ge bond in GeO_4 tetrahedra and the one in 900-970 cm^{-1} range given by the stretching vibration of Si-O-Ge bond are no longer reflected in the Raman spectra after heat

treatment at 1200°C as a result of the separation of phases rich in silicon or germanium respectively.

After 1200^{o}C heat treatment the band arround 3450 cm^{-1} attributed to O-H bond stretching vibration, is not present anymore in the Raman spectra according with the results of differential thermal analysis. The Raman spectrum of the sample with atomic ratio Si/Ge 2:1 shows the typical cristobalite bands, phase identified also by X-ray diffraction [53-65]. The vibrational modes arround 430 cm^{-1} and 490 cm^{-1} can be associated with Q^4 and Q^3 units, respectively [32, 41-47].

The Raman spectra of the 900^{o}C heat treated (30 minutes) samples with atomic ratio Si/Ge 1:1-1:4 are specific to the cristalline structure, clearly evidenced the bands for Ge-O-Ge vibration in GeO_4 tetrahedra arround 450, 525 and 880 cm^{-1} respectively. This results are in according with X-ray diffraction where the GeO_2 phase has been identified.

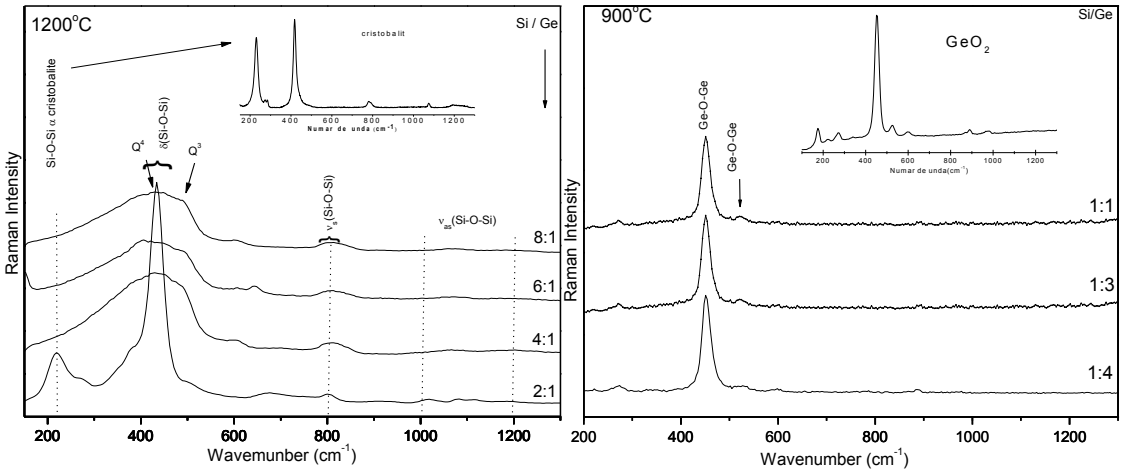

Figure 2.9. Raman spectra for the heat treated samples at 1200/900^{o}C for 30 minutes.

The Raman spectra recorded for the 1200°C heat treated samples for 24 houres, (Figure 2.10), reflect the bands characteristic to the cristobalite crystalline phase, attributed to the antisymmetric and symetric stretching vibration and to the bending vibration of Si-O-Si bond arround 1100 cm^{-1}, 800 cm^{-1}, 430-490 cm^{-1} and ~ 220 cm^{-1}, respectively, according with X-ray diffraction [10, 11, 14-19, 21, 22, 34, 36-39, 52**]**.

For the 1200^{o}C heat treated samples for 30 minutes, the vibration modes at 430 and 490 cm^{-1}can be associated with and the Q^4 and Q^3, respectively [32, 41-47].

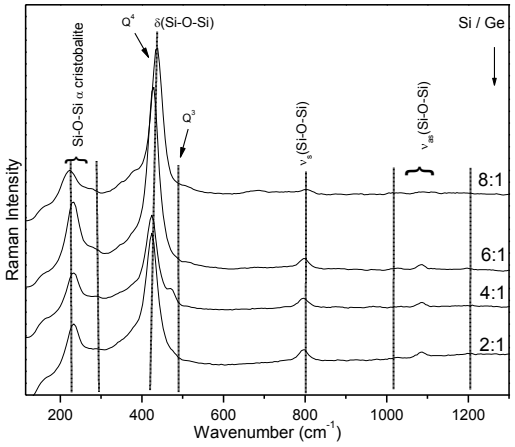

Figure 2.10. Raman spectra for the heat treated samples at 1200°C for 24 houres.

The developments of the Raman spectra at different heat treatments are presented in Figure 2.11 for a better view of the effect of the thermal treatments on the samples structure. Theese analysis indicate the both absence of bands corresponding to C-H bending vibrations and O-H stretching vibration. One can see also the lack of two other bands arround 880 and 980 cm^{-1}, attributed to Ge-O-Ge and Si-O-Ge stretching vibrations, respectively. Spectral behavior evidenced by the heat treatment increasement shows a good dispersion of germanium in the silicate network.

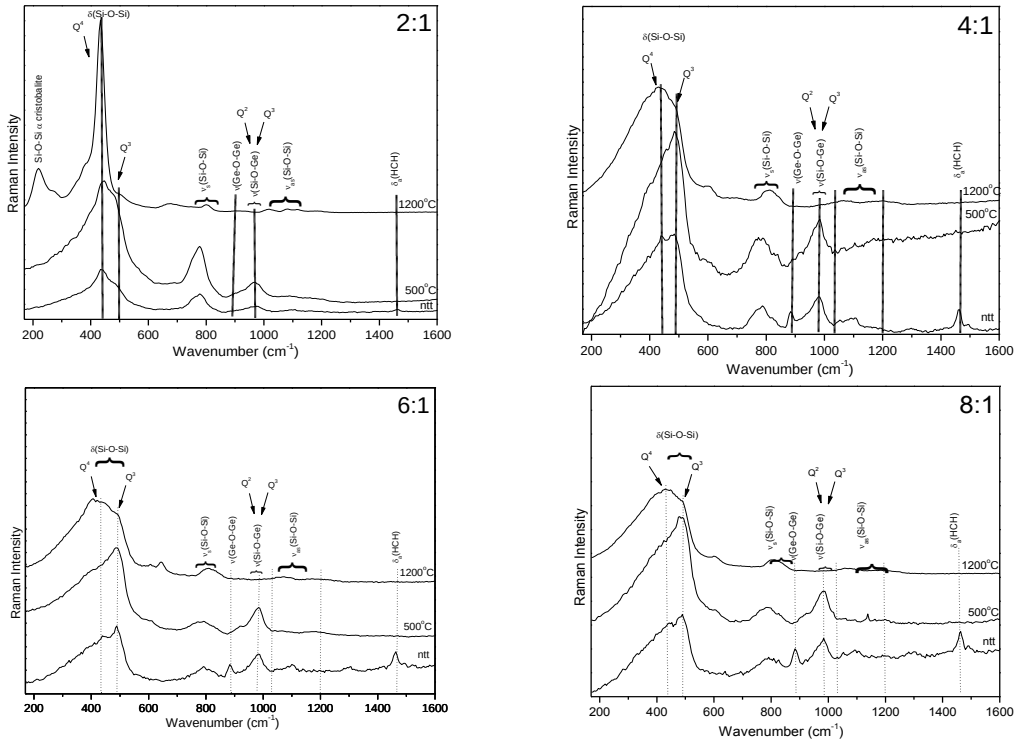

Figure 2.11. Evolution with heat treatement of Raman spectra

2.4. Structural characterization by Infrared spectroscopy

IR absorption spectra recorded for the as-prepared and heat treated samples obtained by sol-gel method, are presented in the range between 400 and 1750 cm^{-1}, the location of spectral bands assigned to SiO_4 and GeO_4 units.

IR spectra of the as-prepared samples are shown in figure 2.12. Broad band from 450 cm^{-1} can be attributed to asymmetric bending vibration of Si-O-Si bonds in the SiO_4 units [14-18, 66-72]. Bands at 520, 550 and 580 cm^{-1} (resolved for samples with a higher germanium content , with Si / Ge ratio between 1:1 - 1:4) are joined in a single line with maximum at 550 cm^{-1} in spectra of the samples with a higher silicon content and can be attributed to bending vibrations of Ge-O-Ge bonds in GeO_4 units [29, 73].

Band at 760 cm^{-1} moves to higher wave numbers (800 cm^{-1}) with increasing silicon content in the samples and is attributed to symmetric stretching vibrations of Si-O-Si linkages between SiO_4 units (Q^4 units) [10, 11, 14-16, 18, 21, 28, 34, 51, 71-75].

The absorption band at 870 cm^{-1} can be attributed to vibrations Ge-O-Ge bonds in GeO_4 units [23, 24, 73, 76, 77]. This intense band for samples with higher germanium content decreases in intensity with increasing silicon content in the sample, while a weak shoulder at 940 cm^{-1} associated with the stretching vibration $Si\text{-}O^-$ bonds in the SiO_4 tetrahedra (Q^2 units) and Si-OH [15, 16, 18, 21, 28, 78-82] that appears in all the as-prepared samples spectrum, increases in intensity with increasing silica content in the samples.

Also note that the band appeared around 960 cm^{-1} assigned to stretching vibrations of Ge-O-Ge linkages in GeO_4 units [73] is found only in spectra of samples with the Si/Ge ratio 1:1-1:4. Shoulder at 1000 cm^{-1} is assigned to stretching vibration of Si-O-Ge bonds (Q^2 units) [11, 34, 36, 71, 73, 81, 83, 84] and disappears from the spectra as the silicon content increases.

Shoulder at 1040 cm^{-1} in the vicinity of 1080 cm^{-1} band, is attributed to asymmetric stretching vibration of Si-O-Si bonds [11, 17, 34, 36, 67, 71, 74, 75, 81, 83-85] and is observed only for samples with the Si/Ge ratio 1:4, 1:3 respectively. Intense band at 1080 cm^{-1} is attributed to asymmetric stretching vibration of Si-O-Si bonds [10, 11, 14-16, 18, 21, 28, 34, 35, 36, 72, 81, 84-88] (Q^3 units) and the shoulder at 1200 cm^{-1} is associated with asymmetric stretching vibration of Si-O-Si bonds (Q^4 units) [11, 14,

16, 34, 35, 75, 85, 88] . Band at 1635 cm^{-1} is attributed to bending vibrations of OH bonds [15, 16, 18, 23, 28, 35, 71, 72, 88] and the intense broad band at 3430 cm^{-1} to stretching vibrations of OH bonds [11, 15, 18, 30, 35, 36, 72, 81, 83, 88].

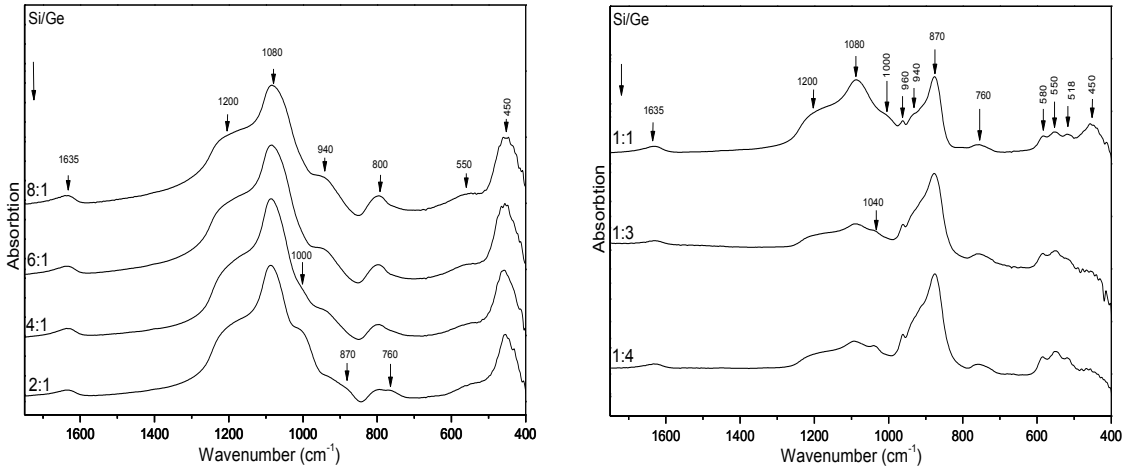

Figure 2.12. IR spectra for the as-prepared samples

IR spectra of heat treated samples for 30 min. at 550°C are shown in figure 2.13. Analyzing the obtained IR absorption spectra we do not observe substantial changes in the shape of spectral lines. The same behavior is observed for the bands at 870 cm^{-1} and 1080 cm^{-1}, which decreases, respectively increase, in intensity with increasing silicon content in the samples.

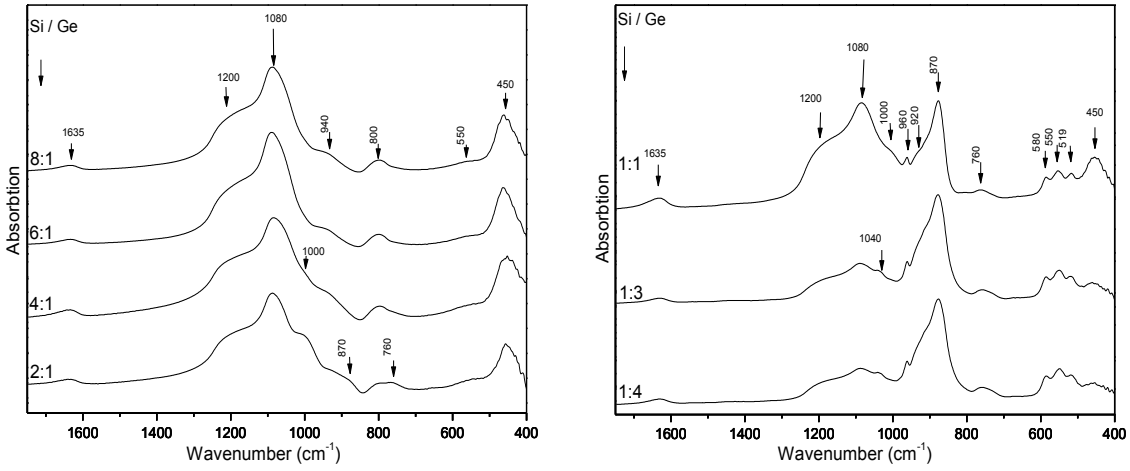

Figure 2.13. IR spectra for the heat treated samples at 550°C for 30 minutes

IR spectra of heat treated samples for 30 minutes at 1200/900°C are shown in figure 2.14. By analyzing the spectra we observed the absorption bands at 670 cm^{-1} and

920 cm^{-1}, especially for samples with higher germanium content, attributed to stretching vibration of Si-O-Ge bond [24, 73]. The same behavior is observed also for the bands at 870 cm^{-1} and 1080 cm^{-1}, which decrease respectively increase in intensity with increasing silica content in the samples and is observed the disappearance of the band at 1635 cm^{-1} and 3430 cm^{-1} respectively, attributed to OH vibrations.

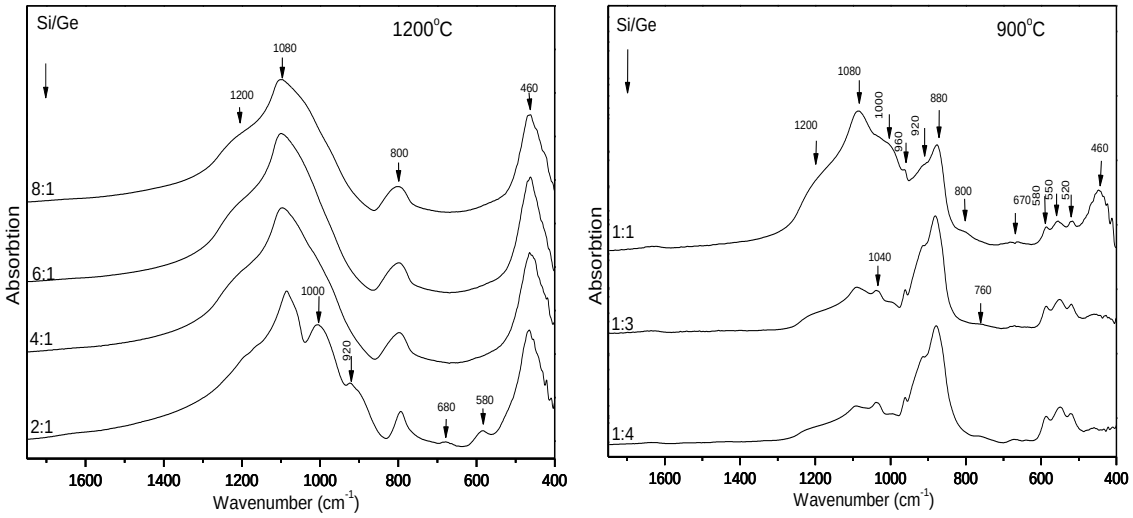

Figure 2.14. IR spectra for the heat treated samples at 1200/900°C for 30 minutes

For a better view of the heat treatment effect for the structure of the samples in figure 2.15 are shown the spectral changes separately for each sample. FTIR data show that the samples undergo structural changes when performing heat treatment, but are most affected by the changes in the Si/Ge ratio.

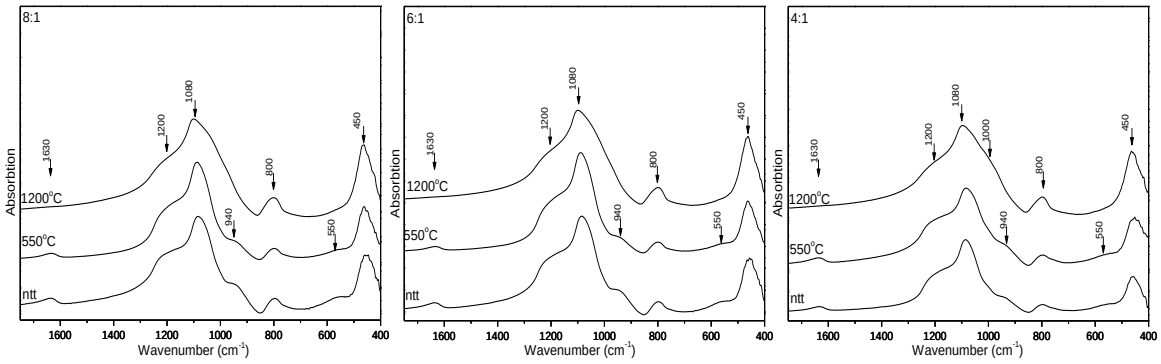

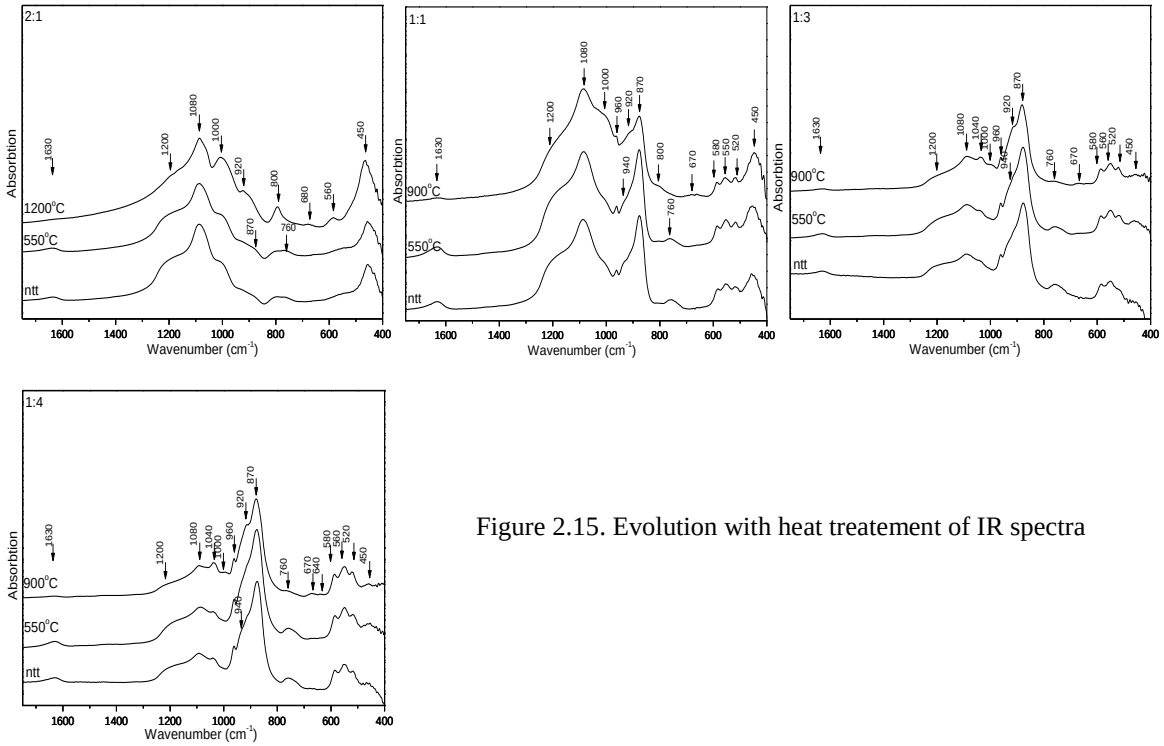

Figure 2.15. Evolution with heat treatement of IR spectra

2.5. Structural characterization by MAS-NMR

Nuclear magnetic resonance spectra (NMR) were recorded for ^{29}Si nucleus from the 0.995 • [(1-x) SiO2 • xGeO2] • 0.005Gd2O3 system on solid samples, as powder. ^{29}Si MAS NMR spectra were processed using the Dmfit program [89]. By changing the Si/Ge ratio and using heat treatment the structural changes that take place are highlighted by the resonance peak positions changes which depend on the coordination of silicon atoms and on the other structural changes that take place in their neighborhood.

^{29}Si MAS NMR spectra of heat-treated samples shown in Figure 2.16, indicates the presence of units Q^4, Q^3 and Q^2 [28, 37, 90, 91]. With increasing silicon content in the sample the Q^4 and Q^3 units tends to equalize. The results obtained by deconvolution for chemical shifts δ (ppm), the Q^n fraction, namely the width of Q^n units are listed in Tables 2, 3 and 4 and plotted in Figure 2.17. Note that with increasing SiO_2 content (Figure 2.17.b), it decreases the number of biding oxygen in the sample, namely the Si-O-Si bridges, decreasing the glass stability. In the vitreous samples with higher silicon content, the number of Si-O-Si bridges decrease and chains of Q^3 units forms, namely bridges of Si-O-Ge (depolymerization occurs). At this stage it is not about a development of crystalline phases, the reorganization process that precedes

crystallization leads to internal tension in samples which is reflected in the shape of these lines, particularly in line broadening associated with Q^2 units.

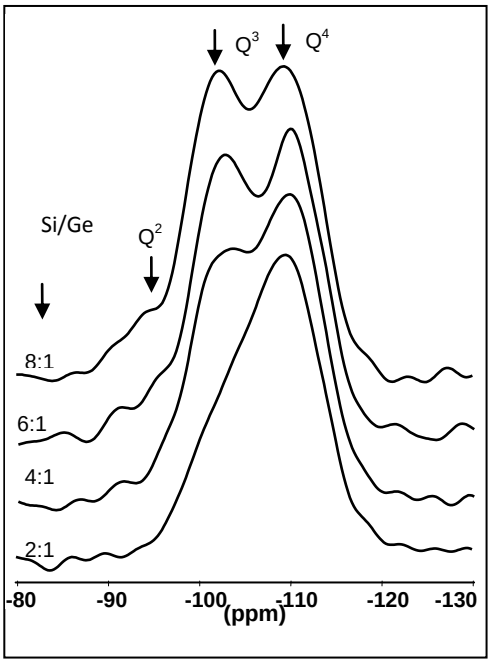

Figure 2.16. The NMR spectra of the as-prepared samples

Table 2. The Q^n position (ppm) function on the samples composition in the as-prepared system

Q^n (ppm) / Si/Ge	Q^2	Q^3	Q^4
2:1	-93.51	-101.75	-109.63
4:1	-91.28	-101.71	-109.88
6:1	-94.90	-102.21	-110.10
8:1	-93.36	-101.49	-109.70

Table 3. The Q^n fraction (%) function on the samples composition in the as-prepared system

Q^n (%) / Si/Ge	Q^2	Q^3	Q^4
2:1	0.11	24.59	75.31
4:1	1.02	42.26	56.72
6:1	3.55	44.50	51.95
8:1	6.12	42.07	51.81

Table 4. The width of Q^n units (ppm) function on the samples composition in the as-prepared system

Q^n (ppm) / Si/Ge	Q^2	Q^3	Q^4
2:1	1.20	7.99	9.36
4:1	2.90	8.10	8.24
6:1	3.68	7.24	6.99
8:1	5.39	7.18	8.24

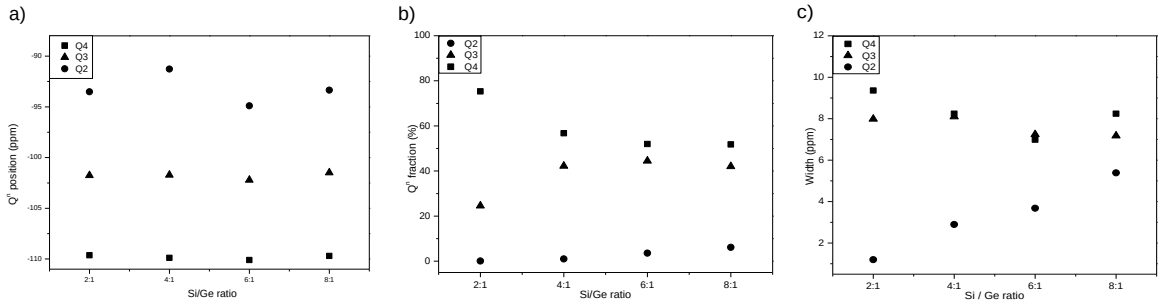

Figure 2.17. a)The Q^n position (ppm), b) Q^n fraction (%), c) width of Q^n units (ppm) function on the samples composition in the as-prepared system

^{29}Si MAS NMR spectra of heat treated samples for 30min. at 550^{o}C, presented in Figure 2.18, indicates mostly the presence of Q^4, Q^3, Q^2 units [28, 37, 90, 91]. The results for chemical shifts δ (ppm) obtained by deconvolution, the Q^n fraction, namely the width Q^n units are presented in tables 5, 6, 7.

After heat treatment at 550°C, the spectrum lines are less resolved; the Q^n fraction is relatively constant showing for all compositions a similar structure, non-crystalline structure solved by a homogeneous distribution of GeO_4 units in silica matrix.

Table 5. The Q^n position (ppm) function on the samples composition in the 30 min heat treated at 550°C system

Q^n (ppm) / Si/Ge	Q^2	Q^3	Q^4
2:1	-92.96	-101.29	-109.09
4:1	-93.86	-100.90	-109.10
6:1	-92.01	-101.11	-109.70
8:1	-92.82	-100.60	-109.01

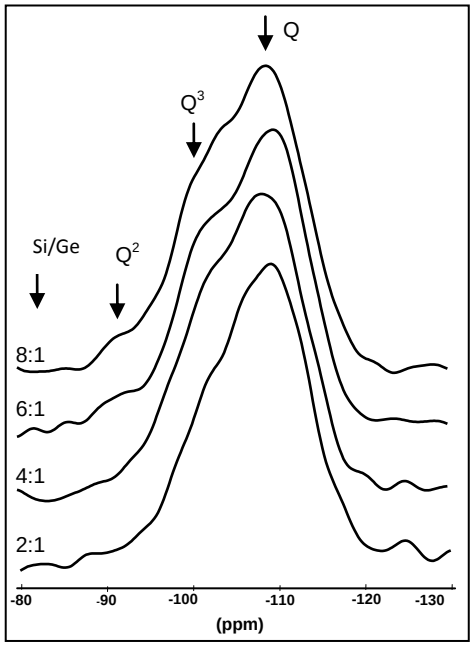

Figure 2.18. The NMR spectra of the 30 min heat treated at 550°C samples

Table 6. The Q^n fraction (%) function on the samples composition in the 30 min heat treated at 550°C system

Q^n (%) / Si/Ge	Q^2	Q^3	Q^4
2:1	1.77	32.91	65.32
4:1	3.25	27.83	68.91
6:1	4.67	29.98	65.35
8:1	5.61	24.12	70.27

Table 7. The width of Q^n units (ppm) function on the samples composition in the 30 min heat treated at 550°C system

Q^n (ppm) / Si/Ge	Q^2	Q^3	Q^4
2:1	2.97	8.17	8.92
4:1	6.66	8.10	10.16
6:1	6.04	7.79	9.53
8:1	6.48	7.46	10.60

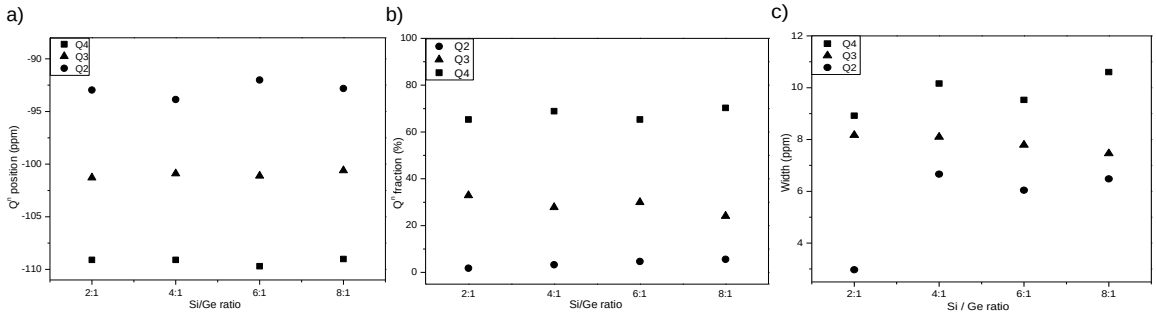

Figure 2.19. a)The Q^n position (ppm), b) Q^n fraction (%), c) width of Q^n units (ppm) function on the samples composition in the 30min. heat treated at 550°C system

^{29}Si MAS NMR spectra of heat treated samples for 30min. at 1200°C, showed in Figure 2.20 indicates mostly the presence of Q^4, Q^3, Q^2 units, except of the Si/Ge ratio 2:1 sample where by deconvolution, two Q^4 units were identified. The chemical shift from ~ -110 ppm corresponds to the still present amorphous silicon phase and from literature it is known that the chemical shift at ~ -107 ppm is attributed to the cristobalite

[92], which is confirmed by X-ray diffraction of the sample. The results for chemical shifts δ (ppm) obtained by deconvolution, the Q^n fraction, namely the width of Q^n units, are contained in tables 8, 9 and 10. Even for these samples the structure is similar after heat treatment, except for the sample with Si/Ge ratio 2:1 where the deconvolution showed a different structure.

Table 8: The Q^n position (ppm) function on the samples composition in the 30 min heat treated at 1200°C system

Q^n (ppm) / Si/Ge	Q^2	Q^3	Q^4	Q^4
2:1	-97.98	-100.71	-111.82	-107.07
4:1	-98.54	-102.78	-110.19	-
6:1	-96.36	-101.96	-110.09	-
8:1	-96.78	-103.90	-110.91	-

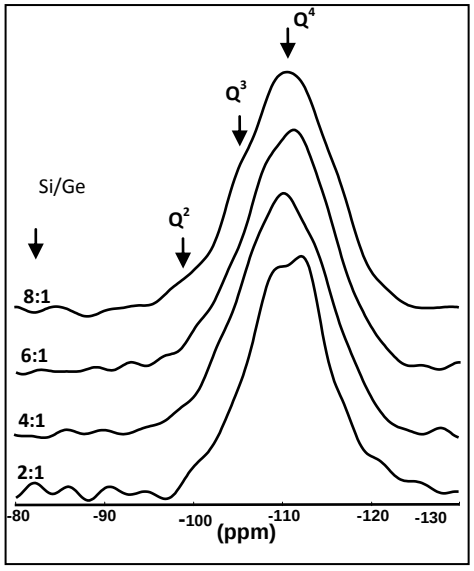

Figure 2.20. The NMR spectra of the 30 min heat treated at 1200°C samples

Table 9. The Q^n fraction (%) function on the samples composition in the 30 min heat treated at 1200°C system

Q^n (%) / Si/Ge	Q^2	Q^3	Q^4	Q^4
2:1	1.12	2.59	37.56	58.73
4:1	1.83	2.89	95.28	-
6:1	0.43	5.72	93.85	-
8:1	1.69	15.53	82.79	-

Table 10. The width of Q^n units (ppm) function on the samples composition in the 30 min heat treated at 1200°C system

Q^n (ppm) / Si/Ge	Q^2	Q^3	Q^4	Q^4
2:1	2.29	3.31	8.90	8.54
4:1	3.60	3.21	10.75	-
6:1	1.98	5.99	10.79	-
8:1	3.68	7.93	9.77	-

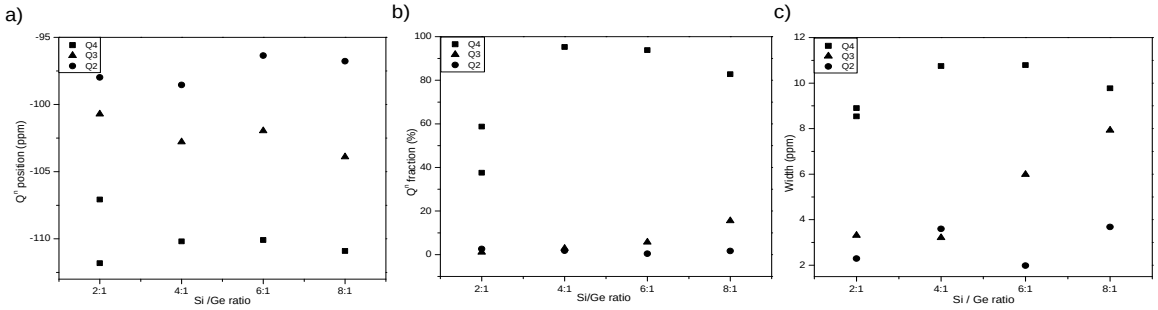

Figure 2.21. a)The Q^n position (ppm), b) Q^n fraction (%), c) width of Q^n units (ppm) function on the samples composition in the 30min. heat treated at 1200°C system

Analyzing the spectral evolution of the samples before and after heat treatment (Figure 2.22), it can be seen that in as-prepared samples the spectra lines are well resolved and

the fraction of Q^3 and Q^4 units tend to equalize with increasing the amount of silica in the samples. After treatment at 550°C, respectively 1200°C, the spectral lines are less resolved, a similar structure being observed, except the sample with Si/Ge ratio 2:1.

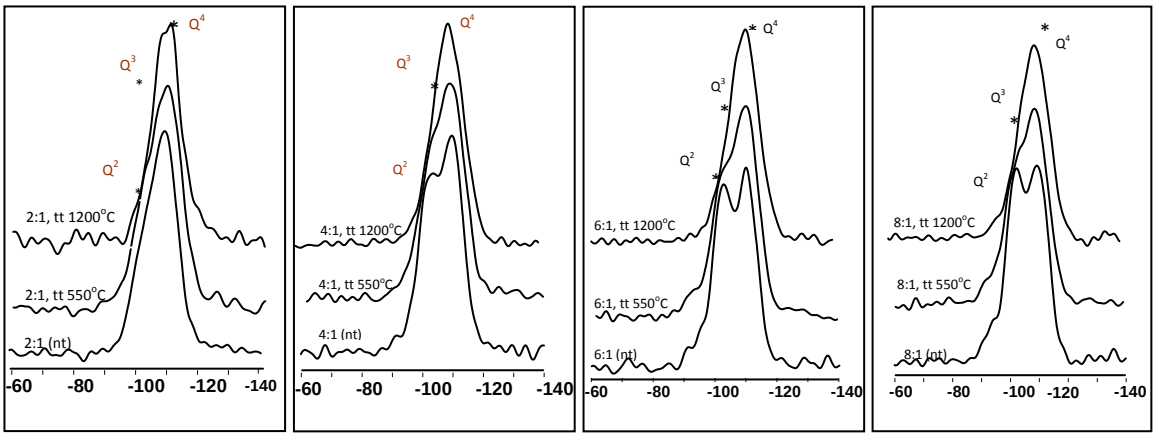

Figure 2.22: The NMR spectra function on their thermal history

In conclusion, the spectra with thermal treatments tend to be less resolved, the differentiation of Q^n units becoming less visible. There are no changes once with the germanium addition concerning the shifts of Q^n units, but an increase in the fraction of Q^3 units with decreasing the amount of germanium it is observed, associated to the growth of hydroxyl groups. Moreover, it is known that the germanium addition do not greatly influences the local neighborhood in silica gel or in the densified glass [22, 91].

3. Experimental results for $0.995 \cdot[(1-x)SiO_2 \cdot xGeO_2]\cdot 0.005\cdot Gd_2O_3$ system obtained by spray-drying method

3.1. Thermal analysis results

Thermal analysis curves for the samples obtained by sol-gel process revealed the removes water and other organic components temperatures and also the others thermal events that occur in the samples. In the figure 3.1 are presented the curves of thermal analysis for the samples obtained by the ratio Si/Ge 6:1 and 1:1 respectively.

The endothermic effect which is attributed to elimination of adsorbed water and solvent is accompanied by weight loss in TGA curve and occurs in the range 60-80°C.

The exothermic effect , occuring in the range 210 - 550^{o}C, is indicating a decomposition of the organic part from the silica matrix, elimination and decomposition of nitrates and chlorides is accompanied on the DTA curve by exothermic effects [8-13].

For samples with higher silicon content (samples with the ratio Si/Ge 8:1-2:1) the phase transition peak is not observed, this samples remain amorphous even after the 900^{o}C heat treatment. For samples with higher germanium content (samples with the ratio Si/Ge 1:1-1:4) the exothermic peaks in the range 600-800^{o}C correspond probably to a phase transition and there are not accompanied by weight loss in TGA curve. Following the thermal analysis have been established the heat treatment temperatures to 550^{o}C and 900^{o}C.

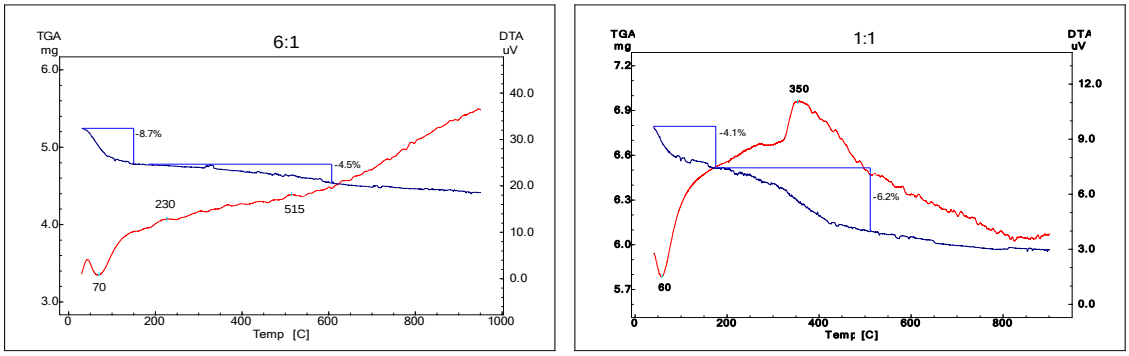

Figure 3.1. DTA and TGA curves for the sample with 6:1and 1:1 Si/Ge ratio

3.2. Structural characterization by XRD

X-ray patterns recorded on as-prepared samples (Figure 3.2) show an amorphous structure, which could be concluded from the broad characteristic diffraction peak between at ~ 2θ ~ 24^{o}, on account of the amorphous character of as-prepared xerogels [13]. The existence of small nanocrystals of a few nanometers is suggested by the presence of large peaks, around 38 and 64 degrees, which is observed in the X-ray patterns of samples with high germanium content [93].

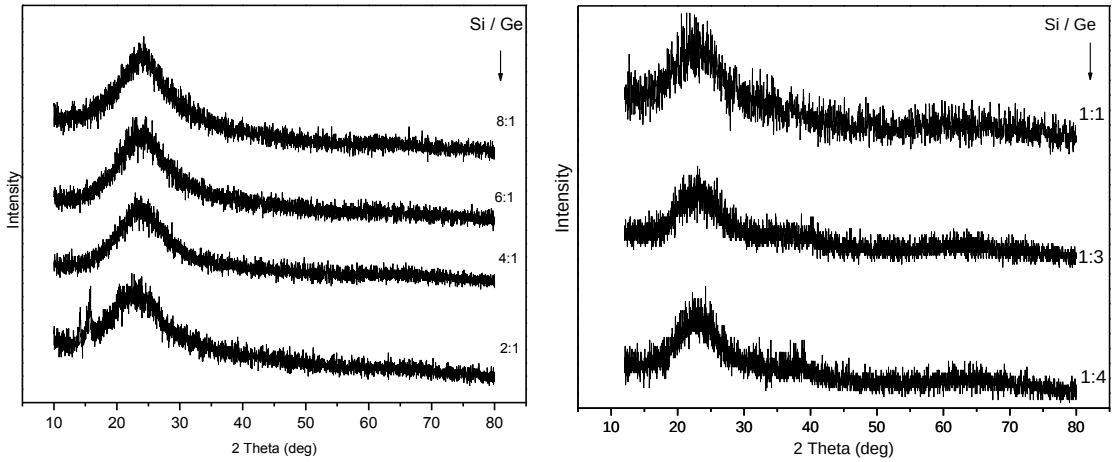

Figure 3.2. X-ray patterns for the as-prepared samples

X-ray patterns of the samples heat treated 30min. at 550^{o}C shown in figure 3.3, presents a broad peak with specific features of non-crystalline systems (samples with the ratio Si/Ge 8:1-2:1).

The X-ray patterns for the samples with 1:1 Si/Ge ratio, the central peak retains its specific features of non-crystalline systems, and for samples with a high germanium content (samples with Si/Ge ratio 1:3, respectively 1:4) present crystalline characteristics and germanium oxide being the identified phase.

The average crystallites size, determined by Scherrer's formula for the peak with $2\theta = 26^{o}$ for this two samples, decreases with increasing germanium content of the sample and is 11.5 nm for the 1:3 Si/Ge ratio sample, respectively 5.7 for the 1:4 sample.

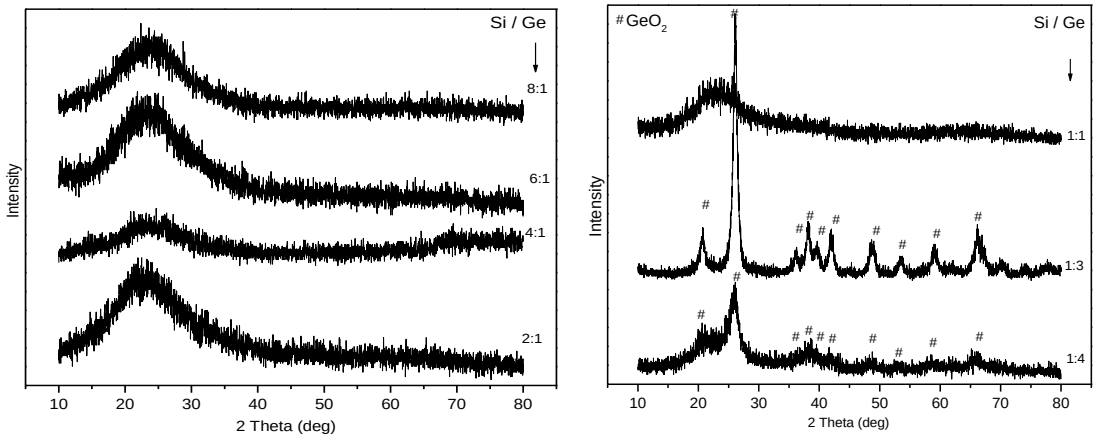

Figure 3.3. X-ray patterns for the samples 550^{o}C heat treated for 30 minutes.

X-ray patterns of the samples heat treated 30min. at 900^{o}C shown in figure 3.4, presents a broad peak with specific features of non-crystalline systems (samples with the

ratio Si/Ge 8:1-2:1). For samples with a high germanium content (samples with Si/Ge ratio 1:1-1:4) present crystalline characteristics and germanium oxide being the identified phase, and the average crystallites size being around 17 nm.

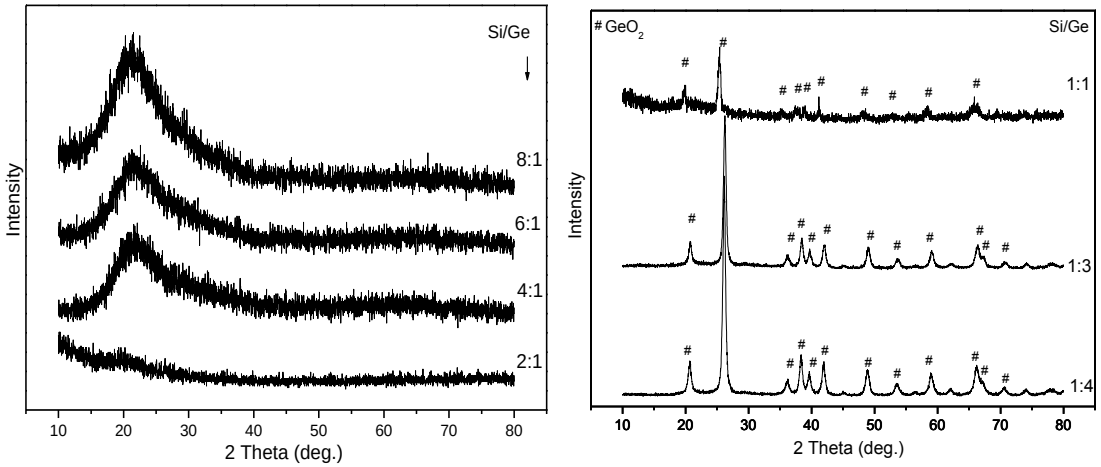

Figure 3.4. X-ray patterns for the samples 900°C heat treated for 30 minutes

3.3. Structural characterization by Raman spectroscopy

The Raman spectra of as-prepared samples (Figure 3.5) with Si/Ge ratio 8:1-2:1 swon broad bands around de 440 cm^{-1}, 800 cm^{-1} şi 1000 cm^{-1} [34, 52], but the fluorescence phenomena covers the Raman signal

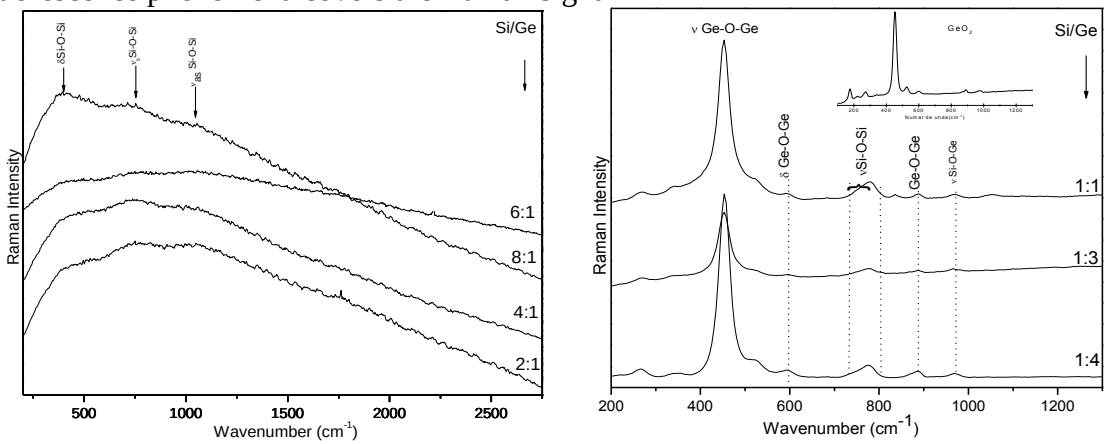

Figure 3.5. Raman spectra for the as-prepared samples

The Raman spectra of as-prepared samples with Si/Ge ratio 1:1-1:4 are specific to the cristalline structure of germanium oxyde and evidenced the bands for Ge-O-Ge vibration in GeO_4 tetrahedra arround 270, 340, 450, 520, 590, respectively 890 cm^{-1} [29, 73], which supports the tendency of segregation observed for these samples in X-ray

patterns (a beginning of nucleation of GeO_2 crystalline phase). The ~ 780cm^{-1} band is attributed to symmetric stretching vibrations of Si-O-Si bond [8, 11, 13-16, 18, 19, 21, 48, 52, 73, 94, 95], and the one from the spectral range of 900-970 cm^{-1} is attributed to ν (Si-O-Ge) [18, 19, 25-27, 30, 32, 33].

The Raman spectra of 30 min. heat treated at 550^{o}C samples are presented in Figure 3.6.

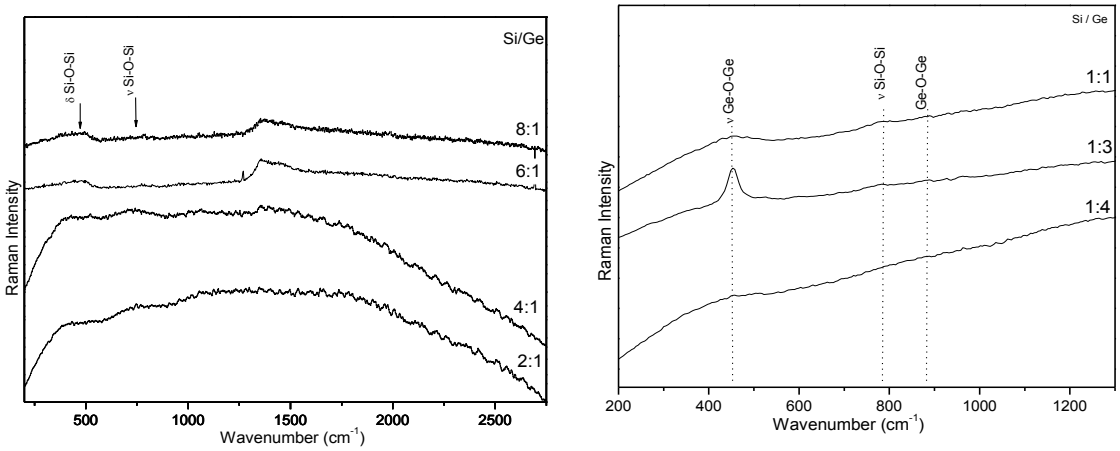

Figure 3.6. The Raman spectra of 30 min. heat treated at 550^{o}C samples

In case of all Raman spectra of 30 minutes heat treated at 550^{o}C samples it is noted that the fluorescence covers the Raman signal. However, we observe some very low intensity bands attributed to the stretching and bending vibrations of the Si-O-Si bond at ~ 430, respectively ~ 780 cm^{-1}, and corresponding vibration bands of Ge-Ge-O bond at 450 cm^{-1}, respectively 880 cm^{-1} [23, 24, 29, 73].

The Raman spectra of 30 min. heat treated at 900^{o}C samples are presented in Figure 3.7.

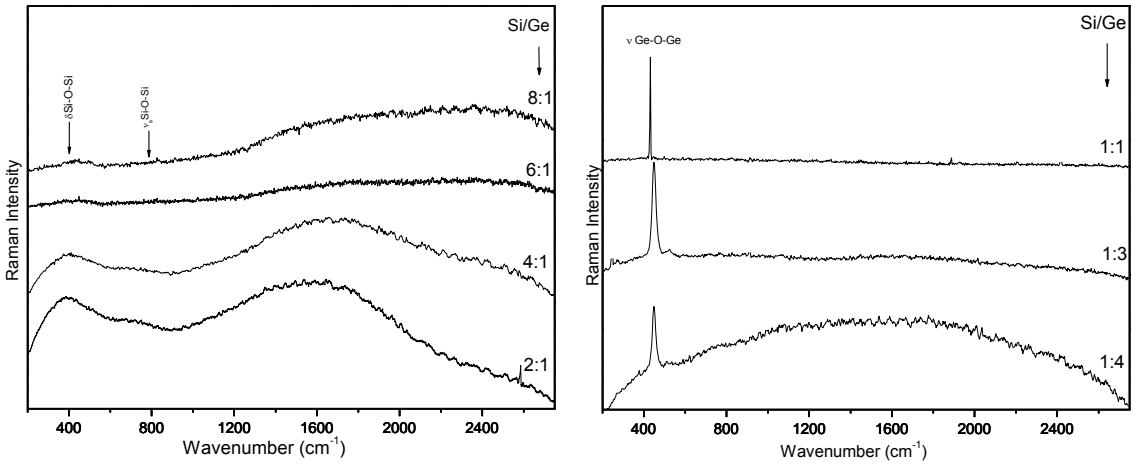

Figure 3.7. The Raman spectra of 30 min. heat treated at 900^{o}C samples

The same thing happens for the Raman spectra of the heat treated samples at 900 ^{o}C for 30 minutes, the phenomenon of fluorescence covering the Raman signal given by these samples. We find, however, in the spectrum the band at 430, respectively 800 cm^{-1} assigned to bending vibrations, respectively the stretching of Si-O-Si bond and the band at 450 cm^{-1} assigned to stretching vibrations of Ge-O-Ge bond in GeO_4.

3.4. Structural characterization by Infrared spectroscopy

IR absorption spectra for as-prepared and heat treated samples obtained by spray-drying method are presented on the range between 400 and 1750 cm^{-1}, where the spectral bands assigned to SiO_4 units, GeO_4 are identified and where structural changes are observed both in composition and heat treatment.

IR spectra of as-prepared samples are shown in Figure 3.8. The wide band from 450 cm^{-1} can be attributed to asymmetric bending vibration of Si-O-Si bounds in the SiO_4 units [14-18, 66-72].

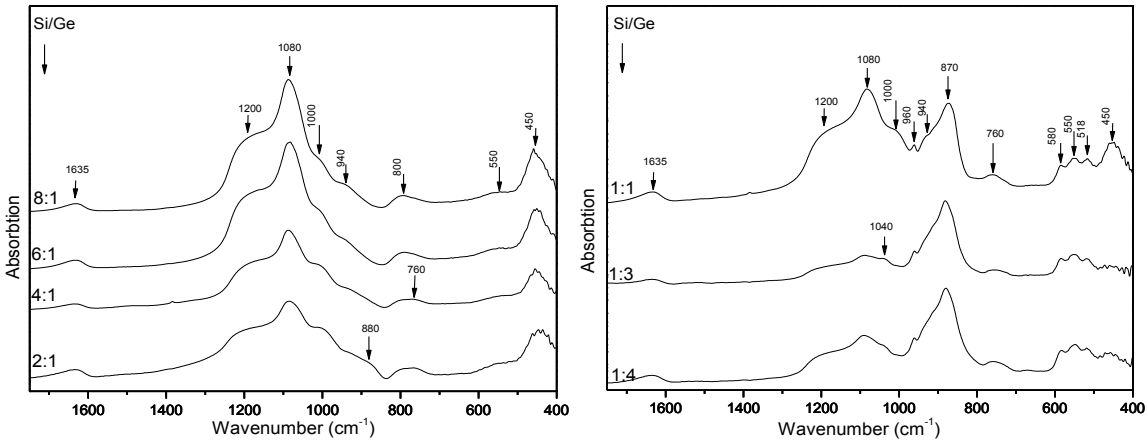

Figure 3.8. The IR spectra of as-prepared samples

The 520 cm^{-1}, 550 cm^{-1}, respectively 580 cm^{-1} bands (visible only for samples with the Si / Ge ratio between 1:1 - 1:4) are joined in a single line with maximum at 550 cm^{-1} in the of the samples with a higher silicon content and can be attributed to bending vibrations of Ge-O-Ge bonds in GeO_4 units [29, 73]. Band at 760 cm^{-1} moves to higher wave numbers (800 cm^{-1}) with increasing silicon content in the samples and is attributed to symmetric stretching vibrations of Si-O-Si linkages between SiO_4 units (Q^4 units) [10, 11, 14-16, 18, 21, 28, 34, 51, 71, 72, 74, 75]. The absorption band at 870 cm^{-1} can be attributed to vibrations Ge-O-Ge bonds in GeO_4 units [23, 24, 73, 76, 77]. This intense

band for samples with higher germanium content decreases in intensity with increasing silicon content in the sample, while a weak shoulder at 940 cm^{-1} associated with the stretching vibration Si-O^- bonds in SiO_4 tetrahedra (Q^2 units) and Si-OH [15, 16, 18, 21, 28, 78-82] that appears in all the as-prepared samples spectra, increases in intensity with increasing silica content in the samples. Also note that the band appeared around 960 cm^{-1} assigned to stretching vibrations of Ge-O-Ge linkages in GeO_4 units [73] is found only in spectra of samples with the Si/Ge ratio 1:1-1:4. Shoulder at 1000 cm^{-1} is assigned to stretching vibration of Si-O-Ge bonds (Q^2 units) [11, 34, 36, 71, 73, 81, 83, 84] and disappears from the spectra as the silicon content increases. Shoulder at 1040 cm^{-1} in the vicinity of 1080 cm^{-1} band, is attributed to asymmetric stretching vibration of Si-O-Si bonds [11, 17, 34, 36, 67, 71, 74, 75, 81, 83-85] and is observed only for samples with the Si/Ge ratio 1:4, 1:3 respectively. The intense band at 1080 cm^{-1} is attributed to asymmetric stretching vibration of Si-O-Si bonds [10, 11, 14-16, 18, 21, 22, 28, 34, 35, 36, 71, 72, 81, 83-88] (Q^3 units) and the shoulder at 1200 cm^{-1} is associated with asymmetric stretching vibration of Si-O-Si bonds (Q^4 units) [11, 14, 16, 34, 35, 75, 85, 88]. Band at 1635 cm^{-1} is attributed to bending vibrations of OH bonds and the intense broad band at 3430 cm^{-1} to stretching vibrations of OH bonds [10, 11, 15, 16, 18, 21, 23, 28, 30, 34-36, 38, 51, 71, 72, 75, 81, 83, 84, 86, 88].

The IR spectra of heat treated samples for 30 min. at 550 °C are shown in Figure 3.99.

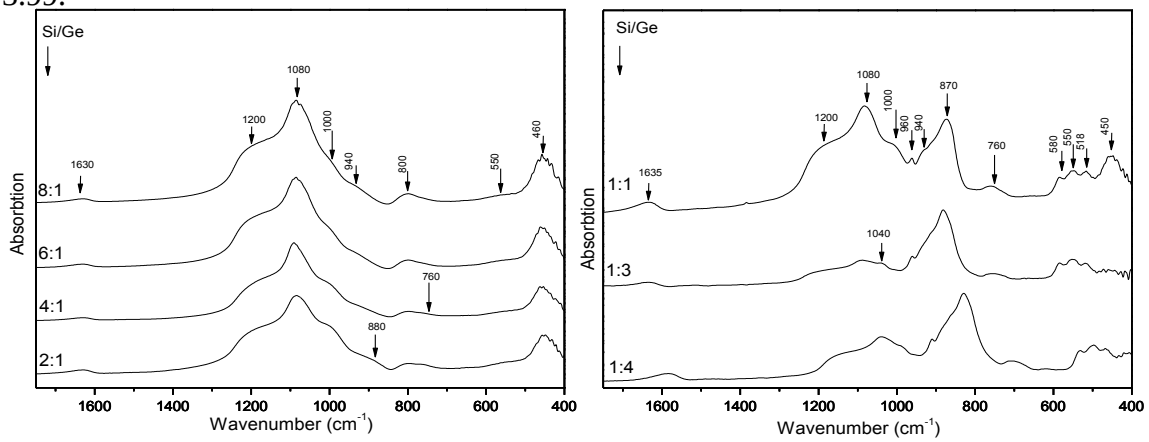

Figure 3.9. The IR spectra of heat treated samples for 30 min. at 550°C

Analyzing the obtained IR absorption spectra there were no new bands observed, the behavior is similar to the as-prepared samples, and the same behavior is observed for

the 870 cm^{-1} and 1080 cm^{-1} bands, which decrease, respectively increased in intensity with increasing silicon content in the samples.

The IR spectra of heat treated samples for 30 min. at 900^{o}C are shown in Figure 3.10. For the samples with higher silica content (Si/Ge ratio between 8:1-2:1) the disappearance of the 940 cm^{-1} shoulder and of the ~ 550 cm^{-1} band is observed, and for the samples with higher germanium content (Si/Ge ratio between 1:1-1:4), absorption bands at 640, 670 cm^{-1} or 920 cm^{-1} are observed due to stretching vibrations of the Si-O-Ge bond units (Q^2 units) [24, 73]. For all the heat treated at 900^{o}C samples, the disappearance of 1635 cm^{-1}band is observed in the spectra corresponding to bending vibrations of OH bonds and the same behavior is observed for 870 cm^{-1}, 1080 cm^{-1} bands which decrease respectively increase in intensity, with increasing silicon content in the samples.

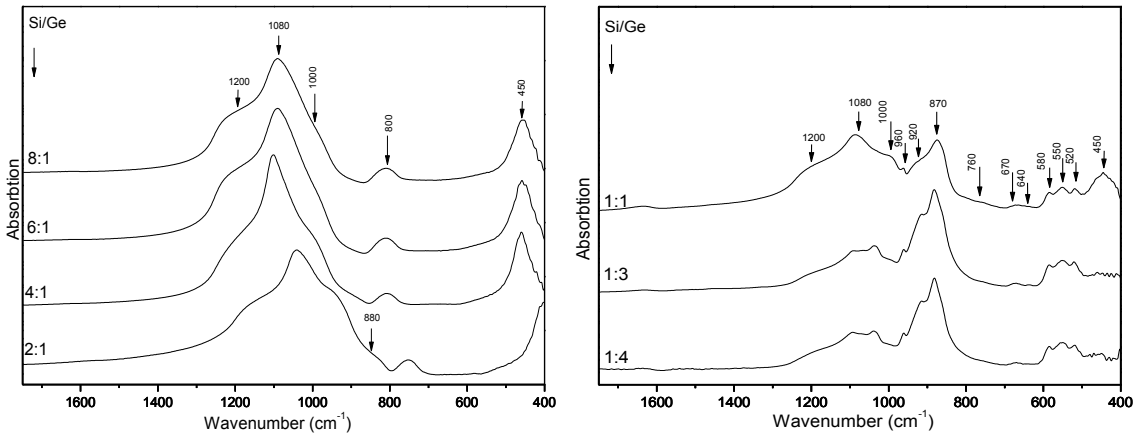

Figure 3.10. The IR spectra of heat treated samples for 30 min. at 900^{o}C

For a better view of the heat treatment effect on samples, in Figure 3.11, spectral developments are highlighted for each sample separately. FTIR data show that the samples undergo structural changes with heat treatment, but are more affected by changes occurred between Si and Ge ratio.

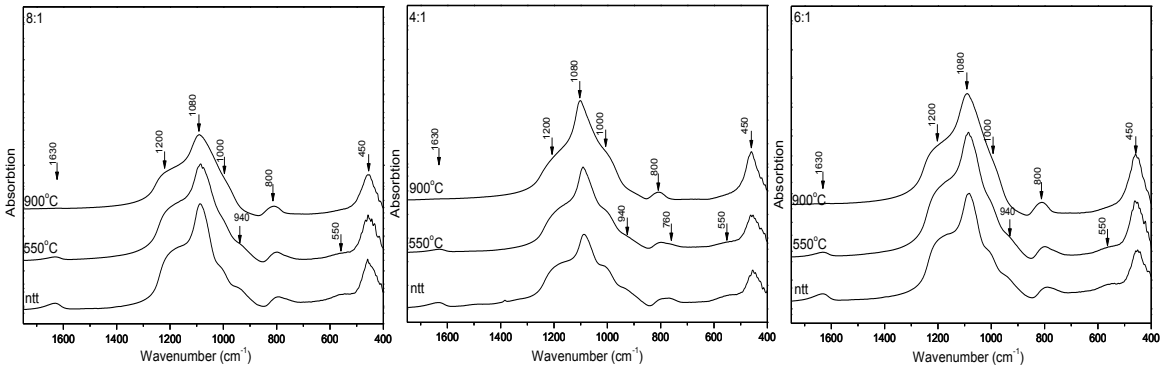

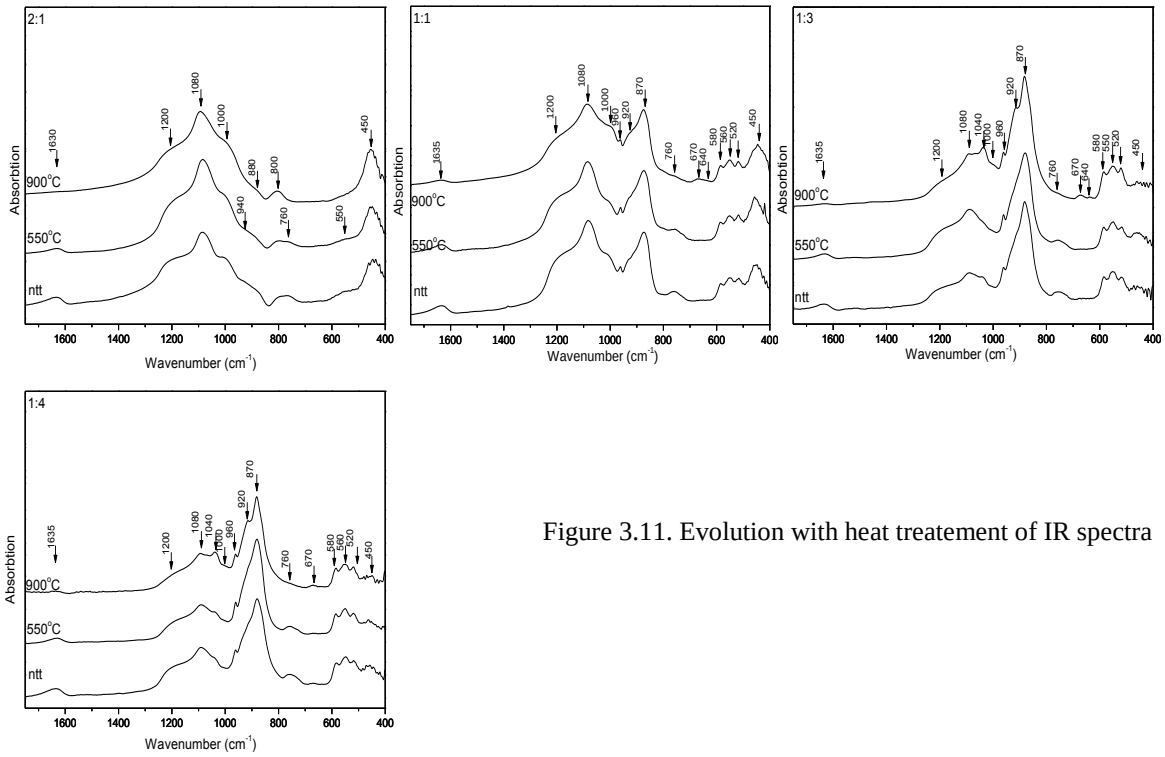

Figure 3.11. Evolution with heat treatement of IR spectra

3.5. Structural characterization by MAS-NMR

The ^{29}Si MAS-NMR spectra of the microspheres belonging to the studied system have broad resonance lines characteristic to amorphous materials and are shown in Figure 3.12. Resonance lines corresponding to structural units Q^2, Q^3 and Q^4 have been identified [28, 37, 90, 91].

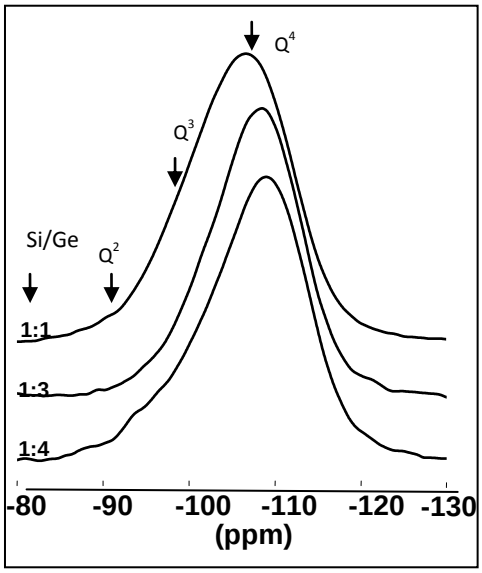

Figure 3.12. The NMR spectra of the as-prepared samples

Table 11. The Q^n position (ppm) of the as-prepared system

Si/Ge \ Q^n (ppm)	Q^2	Q^3	Q^4
1:1	-	-99	-107.17
1:3	-92	-99.74	-108.46
1:4	-94.86	-99.06	-108.95

Table 12. The Q^n fraction (%)of the as-prepared system

Si/Ge \ Q^n (%)	Q^2	Q^3	Q^4
1:1	-	22.33	77.67
1:3	4.88	12.46	82.66
1:4	8.47	9.51	82.02

Table 13. The width of Q^n units (ppm) of the as-prepared system

Si/Ge \ Q^n (ppm)	Q^2	Q^3	Q^4
1:1	-	13.74	12.61
1:3	61.54	9.74	11.03
1:4	13.41	8.98	11.87

The Q^4 fraction is relatively stable with increasing germanium content, while the Q^3 fraction decreases (Figure 3.13.b). For samples with the Si/Ge atomic ratio 1:3 and 1:4, in the resonance spectra besides the Q^4 and Q^3 units we retrieve in addition Q^2 units. The weak polimerization of the silica network in the region of higher germanium content takes place especially at the expense of Q^3 units [93].

The results obtained from spectra deconvolution for chemical shifts δ (ppm), Q^n fraction, respectively the width of Q^n units are listed in Tables 11, 12 and 13. The Q^4 fraction increase slightly with increasing germanium content, while for the samples with the Si/Ge ratio 1:3, respectively 1:4, remains constant and Q^2 fraction decreases with increasing the silicon content.

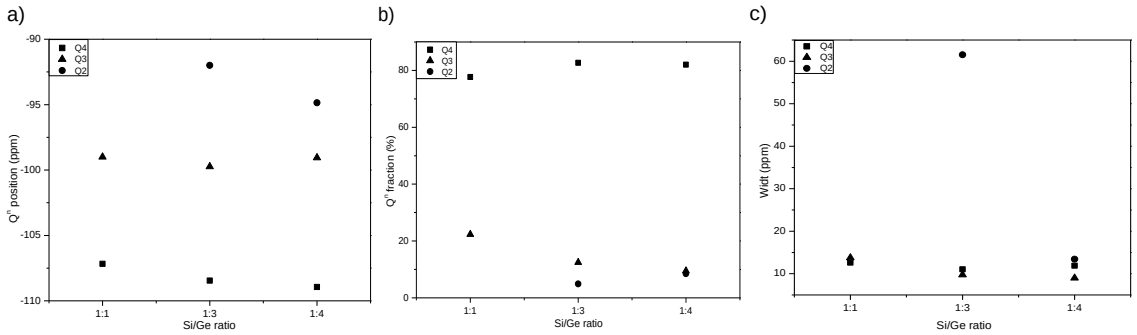

Figure 3.13. a)The Q^n position (ppm), b) Q^n fraction (%), c) width of Q^n units (ppm) function on the samples composition in the as-prepared system

Selected conclusions

By combining the sol-gel and spray drying method, we prepared samples belonging to the 0995 • [(1-x) SiO_2 • xGeO_2] • 0.005Gd_2O_3 system while the atomic ratio was ranged between silicon and germanium, for each method.

DTA

- ✓ Differential thermal analysis was used to determine the thermal evolution of the samples and to determine the optimum heat treatment temperatures.
- ✓ The thermal phenomena shown in the DTA curves were correlated with the structural evolution of the samples. The endothermic peaks were assigned to the removing water process while the exothermic peak was attributed to organic combustion, chlorides elimination and nitrates decomposition.

- For samples prepared by sol-gel method, the temperatures where the transitions to crystalline phases take place were found.
- The endothermic and exothermic peaks are less emphasized for samples prepared by spray-drying method, because this way some of these compounds are eliminated in the preparation.

XRD

- ✓ For samples obtained by sol-gel method we revealed the amorphous nature of the prepared samples to the Si / Ge 1:3 ratio sample.
- ✓ The system obtained by spray-drying method revealed an amorphous character even at high concentrations of germanium due to higher speed in order to obtain powder.
- ✓ Heat treatments lead to the development of nanostructured materials with crystal size between 10-39 nm.
- ✓ Cristobalite nanocrystals have been identified and a small amount of quartz, for samples with a higher silicon content, respectively GeO_2 nanocrystals for samples with a higher germanium content.
- ✓ S-a observat că dimensiunea medie a cristalitelor dezvoltate prin tratamente termice similare în cazul probelor obţinute prin metoda sol-gel este mai mare decât în cazul celor obţinute prin metoda uscării prin pulverizare.

Raman

- ✓ In all Raman spectra it was found the specific vibration bands assigned to Si-O-Si, Si-O-Ge and Ge-O-Ge linkage.
- ✓ After heat treatment at 550 °C, in the spectra of samples with higher silicon content (8:1-2:1) prepared by sol-gel method, the vibration of Ge-O-Ge bond decreases in intensity demonstrating a better insertion of germanium in the amorphous germano-silicate network.
- ✓ After heat treatment at 1200 °C for 30 minutes, and 24 h, we find only the specific vibration bands of Si-O-Si bonds, the spectra being specific to cristobalite, phase identified in X-ray diffraction spectra which shows a good dispersion of germanium inside the network.

- ✓ For the as-prepared and heat treated at 550^{o}C samples with Si/Ge ratio 1:1-1:4, the fluorescence phenomenon covers the Raman signal, and after the 900^{o}C heat treatment the spectra of these samples are specific to germanium oxide.
- ✓ The Raman spectra of the as-prepared and heat-treated samples, prepared by the spray-drying method, with Si/Ge ratio between 8:1-2:1 presents fluorescence which covers the Raman signal.
- ✓ For as-prepared samples with Si/Ge ratio between 1:1-1:4, the Raman spectra are specific to germanium oxide, which supports the tendency towards segregation observed in X-ray diffraction spectra.

IR

- ✓ In all IR spectra we find the specific vibration bands of Si-O-Si, Si-O-Ge and Ge-O-Ge bonds.
- ✓ The bands from 520, 550, 580 cm^{-1} assigned to the deformation vibration of Ge-Ge-O bonds in GeO_4 units are present only in the spectra of samples with a higher germanium content and join in a single line having a maximum at 550 cm^{-1} in spectra of samples with a higher silicon content.
- ✓ FTIR data show that samples undergo structural changes when making heat treatment, being although the most affected by changes in ratio between Si and Ge.

NMR

- ✓ The resonance spectra recorded for the ^{29}Si nucleus revealed Q^2, Q^3, Q^4 units corresponding to SiO_4 structural units.
- ✓ For as-prepared samples obtained by sol-gel method is observed that once with increasing of silicon content decreases the number of oxygen bridges, namely the Si-O-Si bridges, reducing the stability of the glass, forming Q^3 chains units, bridges Si-O-Ge. At this stage it is not about a development of a crystalline phase, but the reorganization process which precedes crystallization leads to an internal tension which is reflected in the form of these lines, particularly in line broadening associated with Q^2 units.
- ✓ After heat treatment at 550 °C, respectively 1200^{o}C for 30 minutes the spectra lines are less resolved, indicating a similar structure for all compositions, a non

crystalline structure solved by a homogeneous distribution of GeO_4 units in the silica matrix, except the sample with Si/Ge ratio 2:1 which presents a different structure.

- ✓ It is noted that with thermal treatments the spectra tend to be less resolved, the differentiation between Q^n units becoming less visible. The germanium addition do not produce shifts of Q^n units position but an increase of Q^3 fraction with decreasing the germanium content from the samples was actually attributed to the growth of the hydroxyl groups.
- ✓ For as-prepared samples obtained by spray-drying method the Q^4 fraction increase slightly with increasing the germanium content in the sample due to decreasing of Q^3 fraction, namely there is a depolymerization of the silica network, and the Q^2 fraction decreases with increasing the silicon content in samples.

Concluzii generale

- ✓ The system was chosen due to its applications in high technology areas of current interest and also for the interest in non-crystalline systems physics with two classical formers of vitreous network.
- ✓ The sol-gel method chosen for synthesis have the advantage of obtaining amorphous homogeneous systems of a high purity for a wide range of concentrations, at temperatures close to room temperature, in comparison with classical melt subcooling method.
- ✓ Using two methods of drying to the same system, leads to compounds with completely different structures.
- ✓ It was noted that the medium crystallites size developed by similar heat treatments for samples obtained by sol-gel method is higher than those obtained by spray-drying method.
- ✓ In both the IR spectra and Raman spectra have been identified the vibration modes associated to Q^2, Q^3, Q^4 units in line with the results obtained following the NMR spectra deconvolution.
- ✓ The spray drying method has the advantage of eliminating from the beginning the organic components that lead to the formation of crystallization germs.

Selected references

1. R.K. Iller, The Chemistry of Silica (Wiley: New-York, 1979)
2. R. Ciceo-Lucacel, Studiul influentei modificatorului de retea vitroasa in sticle pe baza de B_2O_3 asupra starilor locale ale ionilor metalelor de tranzitie, Teza de doctorat, Univ. Babes-Bolyai, Cluj-Napoca (2004)
3. W. S. Roberto, M. M. Pereira, T. P. R. Campos, *Artificial Organs*, 27, 5 (2003) 420.
4. D. Cacaina, R. Viitala, M. Jokinen, H. Ylänen, M. Hupa, S. Simon, *Key Engineering Materials*, 284- 286 (2005) 411-414.
5. C.J. Brinker, N.K. Raman, M.N. Logan, R. Sehgal, R.-A. Assink, D.-W. Hua, T.L. Ward, *Journal of Sol-Gel Science and Technology*, 4 (1995) 117-133.
6. G.Bertrand, P.Roy, C.Filiatre and C. Coddet, Chemical Engineering Science 60, 95 (2005)
7. S. L. Lukasiewicz, *J. Am. Ceram. Soc.*, 2, 4 (1989) 617.
8. M. Crisan, A. Jitianu, D. Crisan, M. Balasoiu, N. Dragan, M. Zaharescu, JOAM Vol. 2, No. 4, 339 – 344 (2000)
9. H. X. Zhang, C. H. Kam, Y. Zhou, X. Q. Han, S. Buddhudu, Y. L. Lam, C. Y. Chan, Thin Solids
10. T. Nakagawa, M. Soga, Journal of Non-Crystalline Solids 260, 167-174 (1999)
11. K. T. Jung, Y.-H. Chu, S. Haam, Y. G. Shul, Journal of Non-Crystalline Solids 298, 193-201(2002)
12. M. Stefanescu, C. Caizer, M. Stoia, O. Stefanescu, JOAM Vol. 7, No. 2, 607 – 614 (2005)
13. M. Popovici, C. Savii, C. Enache, D. Niziiansky, I. Subrt, E. Vecemikova, JOAM Vol. 7, No. 5, 2753 – 2762 (2005)
14. G. N. Barbosa, H. P. Oliveira, Journal of Non-Crystalline Solids 352, 3009-3014 (2006)
15. I. Coroiu, Gh. Borodi, I. Vida Simiti, Al. Darabont, I. Bratu, E. Culea, N. Jumate, JOAM Vol.8, No.2, 529-532 (2006)
16. C. Cannas, M. Casu, A. Lai, A. Musinu, G. Piccaluga, Phys. Chem. Chem. Phys. 4, 2286-2292, (2002)
17. A. Gritco, M. Moldovan, R. Grecu, V. Simon, JOAM Vol.7, No.6, 2845-2847 (2005)
18. G. Liu, G. Hong, J. Wang, X. Dong, Nanotechnology 17, 3134-3138 (2006)
19. C. Duverger, J.-M. Nedelec, M. Benatsou, M. Bouazaoui, B. Capoen, M. Ferrari, S. Turrell, Journal of Molecular Structure 480-481, 169-178 (1999)
20. J. P. Rainho, J. Rocha, L.D. Carlos, R. M. Almeida, J. Mater. Res., Vol.16, No. 8, 2369 – 2376 (2001)
21. X. Luo, C. Zha, B. Luther-Davies, Journal of Non-Crystalline Solids 351, 29-34 (2005)
22. M. May, M. Asomoza, T. Lopez, R. Gomez, Chem. Mater. **9**, 2395-2399 (1977)
23. S. V. Serezhkina, E. A. Tyavlovskaya, G. P. Shevchenko, S. K. Rakhmanov, Journal of Non-Crystalline Solids 351, 35-40 (2005)
24. S. Shibata, T. Kitagawa, F. Hanawa, M. Horiguchik, Journal of Non-Crystalline Solids 88, 345-354 (1986)
25. G.S. Henderson , D.R. Neuville, B. Cochain, L. Cormier, Journal of Non-Crystalline Solids 355, 468–474 (2009)
26. O. Majerus, L. Cormier, D.R. Neuville, L. Galoisy, G. Calas, Journal of Non-Crystalline Solids 354, 2004–2009 (2008)
27. M. Benatsou, M. Bouazaoui, Optics Communications 137, 143-150 (1997)
28. L.A.O'Dell, P.N.Gunawidjaja, M.A.Holland, G.Mountjoy, D.M.Pickup, R.J.Newport, M.E.Smith, J.Solid State NMR 33, 16-24 (2008)
29. E. I. Kamitsos, Y. D. Yiannopoulos, M. A. Karakassides, G. D. Chryssikos, H. Jain, J. Phys. Chem., 100, 11755-11765, (1996)
30. Rajni, K. Pita, S. C. Tjin, S. F. Yu, C. H. Kam, Appl. Phys. A 82, 535-541 (2006)
31. D.-G. Chen, B. G. Potter, J. H. Simmons, Journal of Non-Crystalline Solids 178, 135-147 (1994)
32. H. Aguiar, J. Serra, P. González, B. León, Journal of Non-Crystalline Solids 355, 475–480 (2009)
33. V. Krishnan, S. Gross, S. Muller, L. Armelao, E. Tondello, H. Bertagnolli, J. Phys. Chem. B 111, 7519-7528 (2007)
34. J.Leivo, M.Linden, J.M.Rosenholm, M.Ritola, C.V.Teixeira, E.Levanen, T.A.Mantyla, Journal of the European Ceramic Society 28, 1749-1762 (2008)

35. J.-J. Kim, H.-H. Park, S.-H. Hyun, Thin Solid Films 377-378, 525-529 (2000)
36. T. Nakagawa, T. Hiwatashi, Journal of Non-Crystalline Solids 316, 228-237 (2003)
37. Y-H. Han, A. Taylor, M. D. Mantle, K. M. Knowles, Journal of Non-Crystalline Solids 353, 313–320 (2007
38. X. Xue, J. F. Stebbins, M. Kanzaki, P. F. McMillian, B. Poe, American Mineralogist, Vol.76, 8-26 (1991)
39. M. Ivankovic´, I. Brnardic´, H. Ivankovic´, M. Huskic´, A. Gajovic, Polymer 50, 2544–2550 (2009)
40. G. Encheva, B. Samuneva, P. Djambaski, E. Kashchieva, D. Paneva, I. Mitov, Journal of Non-Crystalline Solids 345&346, 615-619 (2004)
41. C.J. Brinker and G.W.Scherer, Sol-Gel Science: The Physics and Chemistry of Sol- Gel Processing (Academic Press, Inc.: New York, 1990)
42. P. Gonzalez , J. Serra, S. Liste, S. Chiussi, B. Leon, M. Perez-Amor Journal of Non-Crystalline Solids 320, 92–99 (2003)
43. J. González-Hernández, J.F. Pérez-Robles, F. Ruiz, J.R. Martínez, Superficies y Vacío 11, 1 (2000)
44. F.L. Galeener, Phys. Rev. B 19 (8) (1979)
45. H.E. Bergna, The Colloid Chemistry of Silica, Advances in Chemistry, Series 234, American Chemical Society, New York, p.201 (1994)
46. J.P. Borrajo, S. Liste, J. Serra, P. González, S. Chiussi, B. León, M. Pérez-Amor, H.O. Ylänem, M. Hupa, K. Eng. Mat. 254–256, 23 (2004)
47. R.S. Pryce, L.L. Hench, J. Mater. Chem. 14, 2303 (2004)
48. P. Innocenzi, Journal of Non-Crystalline Solids 316, 309-319 (2003)
49. V. Krishnan, S. Gross, S. Muller, L. Armelao, E. Tondello, H. Bertagnolli, J. Phys. Chem. B 111, 7519-7528 (2007)
50. L. Zhang, J. L. Coffer, T. W. Zerda, Journal of Sol-Gel Science and Technology 11, 267-272 (1998)
51. W.Que, L.L.Wang, T.Chen, Z.Sun, X.Hu, J.Sol-Gel Sci. Tech.38, 147:152 (2006)
52. N. Chiodini, A. Paleari, M. Catti, S. Brovelli, D. Di Martino, A. Lauria, R. Lorenzi, G. Spinolo, Solid State Communications 144, 429–432 (2007)
53. J. W. Anthony, R. A. Bideaux, K. W. Bladh, M. C. Nichols, Handbook of Mineralogy, Mineral Data Publishing, Tucson Arizona, USA, by permission of the Mineralogical Society of America (1990)
54. J .Murdoch, Crystallographic notes: cristobalite, stephanite, natrolite, American Mineralogist, 27, 500-506 (1942)
55. W.A. Dollase, Reinvestigation of the structure of low cristobalite, Zeitschrift für Kristallographie, 121, 369-377 (1965)
56. D.P. Peacor, High-temperature single-crystal study of the cristobalite inversion, Zeitschrift für Kristallographie, 138, 274-298 (1973)
57. J.J. Pluth, J.V. Smith, J. Faber, Crystal structure of low cristobalite at 10, 293, and 473 K: Variation of framework geometry with temperature, Journal of Applied Physics, 57, 1045-1049 (1985)
58. D. M. Hatch, S. Ghose, The α-ß transition in cristobalite, SiO_2, Physics and Chemistry of Minerals, 17, 554-562 (1991)
59. R.T. Downs, D.C. Palmer, The pressure behavior of α cristobalite, American Mineralogist, 79, 9-14 (1994)
60. D.C Palmer, L.W. Finger, Pressure-induced phase transition in cristobalite: An X-ray powder diffraction study to 4.4 GPa, American Mineralogist, 79, 1-8 (1994)
61. M.T. Dove, M.S. Craig, D.A. Keen, W.G. Marshall, S.A.T. Redfern, K.O. Trachenko, M.G. Tucker, Crystal structure of the high-pressure monoclinic phase-II of cristobalite, SiO_2, Mineralogical Magazine, 64, 569-576 (2000)
62. L. Huang, M. Durandurdu, J. Kieffer, Transformation pathways of silica under high pressure, Nature Materials, 5, 977-981 (2006)
63. N. Garg, S.M. Sharma, Classical molecular dynamical simulations of high pressure behavior of alpha cristobalite (SiO_2), Journal of Physics: Condensed Matter, 19, 456201 (2007)

64. Y. Liang, C.R. Miranda, S. Scandolo, Tuning oxygen packing in silica by nonhydrostatic pressure, Physical Review Letters, 99, 215504, 1-4 (2007)
65. D. Donadio, R. Martonak, P. Raiteri, M. Parrinello, Influence of temperature and anisotropic pressure on the phase transitions in α-cristobalite, Physical Review Letters, 100, 165502, 1-4 (2008)
66. S. Abiraman, H.K. Varma, T.V. Kumari, P.R. Umashankar, A.John, Bull. Mater. Sci., 25, 5, p.419 (2002)
67. V. Dimitrov, Y. Dimitriev, A. Montenero, J. Non-Cryst. Solids, 180 (1994) 51
68. R.R. Almeida, A.A. Kharlamov, J. Heo, J. Non-Cryst. Solids, 202 (1996) 233
69. R. Iordanova, V. Dimitrov, Y. Dimitriev, D. Klissurski, J. Non-Cryst. Solids, 180 (1994) 58.
70. R. Iordanova, Y. Dimitriev, V. Dimitrov, S. Kassabov, D. Klissurski, J. Non-Cryst. Solids, 231(1998) 227
71. D.Cacaina, H.Ylanen,S.Simon, M.Hupa, J. Mater. Sci: Mater. Med. 19, 1225-1233 (2008)
72. C.-F. Chang, Y-L. Wu, S.-S. Hou, Colloids and Surface A: Physicochem. Eng. Aspects 336, 159-166 (2009)
73. A. Margaryan, M. A. Piliavin, Germanate Glasses: Structure, Spectroscopy, and Properties, Artech House, Boston.London, 1993
74. R.F.S.Lenza, W.L.Vasconcelos, Materials Research, vol.5, nr.4, 497-502 (2002)
75. S.M.Hant, G.S.Attard, R.Riddle, K.M.Ryan, Chem. Mater.17, 1434-1440 (2005)
76. K.U.Joshi, D.Kabiraj, A.M.Narsale, D.K.Avasthi, T.N.Warang, D.C.Kothari, Surface & Coatings Technology 203, 2482-2485 (2009)
77. P. Pernice, A. Aronne, M. Catauro, A. Marotta , J. Non-Crystalline Solids 210 (1997) 23-31
78. Y. Hu, N.H. Liu, U.L. Lin, J. Mater. Science, 33 (1998) 229
79. L. Baia, R. Stefan, W. Kiefer, J. Popp, S. Simon, J. Non-Cryst. Solids, 303 (2002) 379
80. L. Baia, R. Stefan, J. Popp. S. Simon, W. Kiefer, J. Non-Cryst.Solids, 324 (2003) 109 .
81. Y.-H.Han, A.Taylor, M.D.Mantle, K.M.Knowles, J. Non-Crystalline Solids 353, 313-320 (2007)
82. I. Ardelean, S. Cora, R. Ciceo-Lucacel, Mod. Phys. Lett. B, vol.18, no. 16 (2004) 803-810.
83. R.A.Aziz, I.Sopyan, Indian Journal of Chemistry vol.48A, 951-957 (2009)
84. W.Que, L.L.Wang, T.Chen, Z.Sun, X.Hu,Journal of Crystal Growth 288, 75-78 (2006)
85. R.S.Araujo, F.S.Costa, D.A.S.Maia, H.B.Sant'Ana, C.L.Cavalcante Jr., Brazilian Journal of Chemical Engineering vol.24, no.1, 135-141 (2007)
86. M.Ivankovic, I.Brnardic, H.Ivankovic, M.Huskic, A.Gajovic, Polymer 50, 2544-2550 (2009)
87. H.Yamashita, S.Kawasaki, Y.Ichihashi, M.Harada, G.Stewart, M.A.Fox, C.Louis, M.Che, J.Phys.Chem.B 102, 5870-5875 (1998)
88. G.W.Wallidge, R.Anderson, G.Mountjoy, D.M.Pickup, P.Gunawidjaja, R.J.Newport, M.E.Smith, Journal of Materials Science 39, 6743-6755 (2004)
89. D. Massiot, F. Fayon, M. Kapron, I. King, S. Le Calve, B. Alonso, J.-O. Durand, B. Bujoli, Z. Gan, G. Hoatson, Magn. Reson. Chem. 40, 70-76 (2002)
90. H. Marsmann, in: NMR-17, Oxygen-17, and Silicon-29, Ed. P. Diehl, E. Fluck and R. Kosfeld (Springer, Berlin, 1981) pg.65
91. S. Grandi, P. Mustarelli, A. Magistris, M. Gallorini, E. Rizzio, Journal of Non-Crystalline Solids 303, 208-217 (2002)
92. F.J.Stebbins, Mineral Physics and Crzstallographz, Hand-book of Physical Constants, 1995, p.308
93. D.-L. Trandafir, R. V. F. Turcu, Simion Simon, Materials Science and Engineering B 172 (2010) 68–71
94. Ferrer S., Borrás J., Martín Gil J. and Martín Gil F.J. "Thermal studies on sulphonamide derivative complexes". *Thermochim. Acta*, 147, 321 330 (1989); 153, 205 220 (1989); 185, 315 333 (1991)
95. J. Zarzycki, Glasses and the vitreous state, Cambridge University Press, Cambridge (1991)

Acknowledgements

I could have not done the work I presented in this thesis without the help and support I received from many people, whose I would like to acknowledge.

I especially would like to express my deepest gratitude to my supervisor, Prof.dr. Simion Simon, for providing me the opportunity to do my PhD research in his group. Prof.dr. Simion Simon was abundantly helpful and offered invaluable help, assistance, support and guidance. His perpetual energy and enthusiasm in research had motivated all his advisees, including me. In addition, he was always accesible and willing to help me.
Thank you.
I would like to thank Prof.dr. Viorica Simon for encouraging me, for useful discussion, very good advices and excellent collaboration during my research work.
I also want to thank all my professors from Faculty of Physiscs of Babes-Bolyai University who imparted their knowledge during my studies.

Special thanks to all my colleagues from the research group, especially my office colleagues dr. Milica Todea, drd. Maria Maier and dr. Bogdan Frenţiu and my colleague dr. Oana Ponta for their unconditional help, for fruitful discussions and useful suggestions, for their help in making measurements, collaboration, encouragement, friendship and for having good time together both in and out of the laboratory.

Finally, I wold like to express my love and gratitude to my family who always encouraged me and supported me, especially to my mother for her unconditional love, understanding and support and to my little boy, Alexandru, for his understanding and patience during all these years.

Diana Trandafir

Cluj-Napoca, 6 mai 2011